Mathematical Biosciences and Engineering

http://www.aimspress.com/journal/mbe

MBE, 21(4): 5687–5711.
DOI: 10.3934/mbe.2024251
Received: 19 January 2024
Revised: 03 April 2024
Accepted: 08 April 2024
Published: 22 April 2024

Research article

Stability and Hopf bifurcation of an intraguild prey-predator fishery model with two delays and Michaelis-Menten type predator harvest

Min Hou[1], **Tonghua Zhang**[2] **and Sanling Yuan**[1,*]

[1] College of Science, University of Shanghai for Science and Technology, Shanghai 200093, China
[2] Department of Mathematics, Swinburne University of Technology, Hawthorn, Victoria 3122, Australia

* **Correspondence:** Email: sanling@usst.edu.cn.

Abstract: In this paper, we have proposed and investigated an intraguild predator-prey system incorporating two delays and a harvesting mechanism based on the Michaelis-Menten principle, and it was assumed that the two species compete for a shared resource. Firstly, we examined the properties of the relevant characteristic equations to derive sufficient conditions for the asymptotical stability of equilibria in the delayed model and the existence of Hopf bifurcation. Using the normal form method and the central manifold theorem, we analyzed the stability and direction of periodic solutions arising from Hopf bifurcations. Our theoretical findings were subsequently validated through numerical simulations. Furthermore, we explored the impact of harvesting on the quantity of biological resources and examined the critical values associated with the two delays.

Keywords: predator-prey system; Michaelis-Menten type harvesting; delay; Hopf bifurcation; stability

1. Introduction

Lotka and Volterra introduced a system of differential equations known as the Lotka-Volterra equations, which have served as a foundation for studying predator-prey dynamics in ecology [1–3]. Intraguild predation, an ecological phenomenon where competition and predation coexist in the food web, has garnered significant attention for its profound influence on populations, impacting their abundance, distribution, and even evolution [4–6]. In a seminal paper, Polis et al. [7] initially introduced a concept involving a two-species predator system, where one species consumes the other while they compete for shared resources. Subsequent scholars have made substantial advancements in this area [8]. For instance, Hart [9] focused on marine ecosystems, investigating top-down and bottom-up characteristics in model food webs to explain outcomes observed in trophic cascade

experiments in lakes. Moeller et al. [10] proposed a mathematical model demonstrating how two plankton species, acting as mixotrophs, can coexist through resource competition. Safuan et al. [11] developed an intraguild predation model where resources are shared among predators and prey, introducing a carrying capacity proportional to biological resources. Resource availability, impacted by both predators and prey, plays a crucial role in system behavior [12–14]. Abundant and high-quality resources lead to stability, while scarce or degraded resources result in chaotic dynamics, limit cycles, or even chaos [15, 16].

External factors such as harvesting also influence this ecological interaction [17, 18]. Harvesting's impact on resource and fishery management is significant both economically and ecologically [19, 20]. Chaudhuri [21] examined harvesting in the context of two competing species, providing a detailed analysis of equilibrium solutions. Das et al. [22] explored bioeconomic fish extraction in predator-prey fishery models, while Ang and Safuan [23] considered independent harvesting strategies for predators and prey with their own economic values. To address limitations of the unit harvest concept, Clark introduced Michaelis-Menten-type harvesting [24]. Research on the combination of this harvesting type in ecological models has revealed various bifurcation behaviors [25–27]. Sharif and Mohd [28] conducted a comprehensive analysis of harvesting and enrichment effects on intraguild predator fishery ecosystems, highlighting diverse dynamic behaviors.

In predator-prey systems, factors like food digestion, gestation, disease transmission, capture, and defense involve time delays [29–31]. Time delay differential equations exhibit intricate dynamics, especially when delays exceed a critical threshold, leading to Hopf bifurcation and oscillations in population sizes [32, 33]. For example, Li et al. [34] investigated spatial memory and Allee effects in prey-predator systems with time delays. Other researchers have explored various delays and analyzed local stability, Hopf bifurcation, and stability paths using methods like the center manifold and paradigm theory [35–37].

To our knowledge, prior research has not explored a double-delayed predator-prey model with a Michaelis-Menten-type harvesting. This article specifically focuses on gestation delays in prey and predator populations. In Section 2, we establish the model's framework. Section 3 examines equilibrium points and their local stability under varying time delays, including Hopf bifurcation analysis. Section 4 investigates conditions affecting bifurcation direction and stability factors crucial to Hopf bifurcation. In Section 5, we employ numerical simulations to explore the system's complex behavior. Finally, we summarize key findings, draw conclusions, and discuss the significance of our analytical results to conclude the paper in Section 6.

2. Model description and equilibrium

Ang and Safuan in [27] presented an intricate ecological model that comprehensively captures the complex interplay among different species and their respective habitats:

$$\begin{cases} \dfrac{\mathrm{d}X}{\mathrm{d}t} = r_1 X\left(1 - \dfrac{X}{mZ}\right) - aXY, \\ \dfrac{\mathrm{d}Y}{\mathrm{d}t} = r_2 Y\left(1 - \dfrac{Y}{nZ}\right) + bXY - \dfrac{cEY}{d_1 E + d_2 Y}, \\ \dfrac{\mathrm{d}Z}{\mathrm{d}t} = Z(g - uX - vY). \end{cases} \tag{2.1}$$

This model not only elucidates the dynamics of predator and prey but also incorporates the dimension of human predation on the predator species, where $X(t)$ and $Y(t)$ denote the populations of a prey species and predator species over time, respectively. r_1 and r_2 represent the intrinsic growth rates of the prey, denoted as X, and the predator, denoted as Y, respectively. In this context, Z is used to signify a shared resource accessible to both prey and predator populations, with growth rates of m and n, respectively ($0 < m < 1, 0 < n < 1$), satisfying the constraint $m + n = 1$. The parameter g characterizes the growth rate of biotic resources, and u and v represent the consumption rates of resources by prey and predator species, respectively. Furthermore, parameters a and b quantify the strength or intensity of the interaction between the prey and predator species. The catchability coefficient of predator fish is denoted as c, while E represents the harvesting effort applied to predator fish, with d_1 and d_2 as positive constants.

The primary focus of this work centered on exploring the long-term behavior of the system, utilizing the harvest of predator fish as a bifurcation parameter and examining the associated economic implications using Pontryagin's maximum principle. The bistable behavior within the system was leveraged to derive the optimal threshold for predator harvest, aiming to strike a balance between maintaining fishery resources and maximizing economic profit. In this study, our objective was to delve into an unexplored aspect of system dynamics, with a particular emphasis on the impact of time delays. We have thoroughly investigated the predator-prey model within an intraguild setting, incorporating the Michaelis-Menten harvest style and introducing two significant time delays. A key highlight of our research lied in our careful consideration of the gestation time delays for both predator and prey. This approach represents a promising avenue for gaining deeper insights into ecological relationships and mechanisms that yields the following model:

$$\begin{cases} \dfrac{\mathrm{d}X}{\mathrm{d}T} = r_1 X\left(1 - \dfrac{X(T-T_1)}{mZ(T-T_1)}\right) - aXY, \\ \dfrac{\mathrm{d}Y}{\mathrm{d}T} = r_2 Y\left(1 - \dfrac{Y(T-T_2)}{nZ(T-T_2)}\right) + bXY - \dfrac{cEY}{d_1E + d_2Y}, \\ \dfrac{\mathrm{d}Z}{\mathrm{d}T} = Z(g - uX - vY). \end{cases} \tag{2.2}$$

Here, the constants T_1 and T_2 account for the gestation time delays of X and Y, respectively. $T_1(T_2)$ represents the gestation delay in the presence of the prey (predator), i.e., after consuming the shared resource, the prey X (the predator Y) takes some time to convert the shared resource Z into prey (predator) biomass [38]. Now, let's introduce dimensionless variables: $x = anX/mr_2$, $y = aY/r_2$, $z = anZ/r_2$, and $t = r_2T$ so we obtain the following dimensionless system:

$$\begin{cases} \dfrac{\mathrm{d}x}{\mathrm{d}t} = \alpha x\left(1 - \dfrac{x(t-\tau_1)}{z(t-\tau_1)}\right) - xy, \\ \dfrac{\mathrm{d}y}{\mathrm{d}t} = y\left(1 - \dfrac{y(t-\tau_2)}{z(t-\tau_2)}\right) + \beta xy - \dfrac{\delta y}{\sigma + y}, \\ \dfrac{\mathrm{d}z}{\mathrm{d}t} = z(\rho - \varepsilon x - \mu y), \end{cases} \tag{2.3}$$

where the dimensionless parameters are $\alpha = r_1/r_2$, $\beta = bm/an$, $\delta = acE/d_2r_2^2$, $\rho = g/r_2$, $\varepsilon = mu/an$ and $\mu = v/a$. To ensure that the system is biologically feasible, it is assumed that all the parameters are

positive. By the biological senses, the initial conditions are chosen as

$$x(\theta) = \phi_1(\theta) \geq 0, y(\theta) = \phi_2(\theta) \geq 0, z(\theta) = \phi_3(\theta) \geq 0, \phi_i \geq 0, i = 1, 2, 3, \theta \in [-\tau, 0], \tag{2.4}$$

where $\tau = \max\{\tau_1, \tau_2\}, (\phi_1(\theta), \phi_2(\theta), \phi_3(\theta) \in C([-\tau, 0], R_+^3)$ is a continuous vector function in the Banach space mapping $[-\tau, 0] \to R_+^3$ and $R_+^3 = \{(x_1, x_2, x_3) : x_i \geq 0, i = 1, 2, 3\}$.

Notice that in the absence of delays, i.e., $\tau_1 = \tau_2 = 0$, model (2.3) is reduced to the one considered by Sharif and Mohd in [28]. Since the presence of delays does not affect the number and existence of equilibria, we can have the following lemma (see [28] for details).

Lemma 2.1. *For model* (2.3) *with* $\tau_1 = 0$ *and* $\tau_2 = 0$*, the following statements are true.*

(a) If $\mu\sigma + \rho - \delta\mu > 0$*, there is a prey-free equilibrium* $E_1 = \left(0, \frac{\rho}{\mu}, \frac{\rho(\mu\sigma+\rho)}{\mu(\rho+\mu\sigma-\delta\mu)}\right)$*, which is locally stable provided* $\rho - \alpha\mu > 0$ *and* $(\rho + \mu\sigma)^2 - \delta\mu^2\sigma - 2\delta\mu\rho > 0$ *hold.*

(b) There is always a predator-free equilibrium $E_2 = \left(\frac{\rho}{\varepsilon}, 0, \frac{\rho}{\varepsilon}\right)$*, which is locally stable provided* $\delta\varepsilon - \beta\rho\sigma - \varepsilon\sigma > 0$ *holds.*

(c) Coexistence equilibrium E^* *is given by the expression:* $E^* = \left(\frac{\rho-\mu\hat{y}}{\varepsilon}, \hat{y}, \frac{\alpha(\mu\hat{y}-\rho)}{\varepsilon(\hat{y}-\alpha)}\right)$*, where* $\hat{y}$ *is the positive solution to the cubic equation* $A\hat{y}^3 + B\hat{y}^2 + C\hat{y} + D = 0$*, satisfying* $\rho - \mu\hat{y} > 0$ *and* $\alpha - \hat{y} > 0$*. Here,*

$$A = \alpha\beta\mu^2 + \varepsilon^2,\ B = \alpha\beta\mu^2\sigma + \varepsilon^2\sigma - 2\alpha\beta\mu\rho - \alpha\varepsilon^2 - \alpha\varepsilon\mu,$$
$$C = \alpha\beta\rho^2 + \alpha\delta\varepsilon\mu + \alpha\varepsilon\rho - 2\alpha\beta\mu\rho\sigma - \alpha\varepsilon^2\sigma - \alpha\varepsilon\mu\sigma,\ D = \alpha\beta\rho^2\sigma + \alpha\varepsilon\rho\sigma - \alpha\delta\varepsilon\rho.$$

It has been revealed in [28] that in the absence of delay, model (2.3) can have up to three possible equilibria and exhibit complex dynamics, including tri- or bistability phenomena and multi-type bifurcations. In this paper, we will turn our main attention to the investigation of the effects of delay on the dynamics of model (2.3).

3. Local stability and Hopf bifurcation

In this section, we will explore the local stability of the equilibrium point/s of model (2.3), as well as investigate whether or not a Hopf bifurcation can occur at any arbitrary equilibrium point where coexistence is achieved. By linearizing model (2.3), we can derive the characteristic equation at the equilibrium point $E_*(x_*, y_*, z_*)$. This equation determines the behavior of the system near the equilibrium point and provides insight into the stability properties of the system. The representation of the characteristic equation can be stated as follows:

$$\det\begin{pmatrix} \lambda - \alpha + y_* + \dfrac{\alpha x_*}{z_*}(e^{-\lambda\tau_1} + 1) & x_* & -\dfrac{\alpha x_*^2}{z_*^2}e^{-\lambda\tau_1} \\ -\beta y_* & \lambda - 1 - \beta x_* + \dfrac{\delta\sigma}{(\sigma + y_*)^2} + \dfrac{y_*}{z_*}(e^{-\lambda\tau_2} + 1) & -\dfrac{y_*^2}{z_*^2}e^{-\lambda\tau_2} \\ \varepsilon z_* & \mu z_* & \lambda - \rho + \varepsilon x_* + \mu y_* \end{pmatrix} = 0. \tag{3.1}$$

According to (3.1), we first study the local stability of the prey-free equilibrium E_1 and the predator-free equilibrium E_2.

Theorem 3.1. *Consider system* (2.3) *for any* $\tau_1 > 0$ *and* $\tau_2 > 0$*. We have*

(i) If there exists a prey-free equilibrium E_1 (i.e., $\mu\sigma + \rho - \delta\mu > 0$), the prey-free equilibrium $E_1 = \left(0, \frac{\rho}{\mu}, \frac{\rho(\mu\sigma+\rho)}{\mu(\rho+\mu\sigma-\delta\mu)}\right)$ is stable when $\rho - \alpha\mu > 0$ and $0 < \tau_1 < \tau_{2_0}$. Otherwise, it is unstable.

(ii) If $\varepsilon\delta - \varepsilon\sigma - \beta\rho\sigma > 0$ and $0 < \tau_1 < \tau_{1_0}$, the predator-free equilibrium $E_2 = \left(\frac{\rho}{\varepsilon}, 0, \frac{\rho}{\varepsilon}\right)$ is stable. Otherwise, it is unstable.

Proof. (i) If the feasible criterion of $\mu\sigma + \rho - \delta\mu > 0$ is met, equilibrium E_1 always exists. The characteristic equation (3.1) at E_1 is of the form

$$(\lambda - \alpha + \frac{\rho}{\mu})\left[\lambda^2 - \frac{\rho\delta\mu}{(\mu\sigma+\rho)^2}\lambda - \frac{\mu\sigma+\rho-\delta\mu}{\mu\sigma+\rho}(\lambda-\rho)e^{-\lambda\tau_2}\right] = 0. \tag{3.2}$$

Obviously, $\alpha - \frac{\rho}{\mu}$ is one root of Eq (3.2). Let $\mathfrak{G}(\lambda) := \lambda^2 - \frac{\rho\delta\mu}{(\mu\sigma+\rho)^2}\lambda - \frac{\mu\sigma+\rho-\delta\mu}{\mu\sigma+\rho}(\lambda-\rho)e^{-\lambda\tau_2}$ and assume that $\lambda = i\omega(\omega > 0)$ is a root of $\mathfrak{G}(\lambda) = 0$. Then it follows that

$$\begin{cases} \frac{\mu\sigma+\rho-\delta\mu}{\mu\sigma+\rho}\rho\cos(\omega\tau_2) - \frac{\mu\sigma+\rho-\delta\mu}{\mu\sigma+\rho}\omega\sin(\omega\tau_2) = \omega^2, \\ \frac{\mu\sigma+\rho-\delta\mu}{\mu\sigma+\rho}\omega\cos(\omega\tau_2) + \frac{\mu\sigma+\rho-\delta\mu}{\mu\sigma+\rho}\rho\sin(\omega\tau_2) = -\frac{\rho\delta\mu}{(\mu\sigma+\rho)^2}\omega, \end{cases} \tag{3.3}$$

which leads to

$$\omega^4 + \left[\frac{\rho^2\delta^2\mu^2}{(\mu\sigma+\rho)^4} - \left(\frac{\mu\sigma+\rho-\delta\mu}{\mu\sigma+\rho}\right)^2\right]\omega^2 - \frac{(\mu\sigma+\rho-\delta\mu)^2}{(\mu\sigma+\rho)^2}\rho^2 = 0. \tag{3.4}$$

Notice that when $-\frac{(\mu\sigma+\rho-\delta\mu)^2\rho^2}{(\mu\sigma+\rho)^2} < 0$, Equation (3.4) has a unique positive root $\omega_0^2 = \frac{1}{2}\left[\left(\frac{\mu\sigma+\rho-\delta\mu}{\mu\sigma+\rho}\right)^2 - \frac{\rho^2\delta^2\mu^2}{(\mu\sigma+\rho)^4} + \sqrt{\Delta_1}\right]$, where $\Delta_1 = \left[\left(\frac{\mu\sigma+\rho-\delta\mu}{\mu\sigma+\rho}\right)^2 - \frac{\rho^2\delta^2\mu^2}{(\mu\sigma+\rho)^4}\right]^2 + \frac{4(\mu\sigma+\rho-\delta\mu)^2\rho^2}{(\mu\sigma+\rho)^2}$. Substituting ω_0^2 into Eqs (3.3), we obtain

$$\tau_{2_n} = \frac{1}{\omega_0}\left\{\arccos\frac{\omega_0^2\left[\rho - \frac{\rho\delta\mu}{(\mu\sigma+\rho)^2}\right]}{\frac{\mu\sigma+\rho-\delta\mu}{\mu\sigma+\rho}(\rho^2+\omega_0^2)} + 2n\pi\right\}, n = 0, 1, 2, \ldots. \tag{3.5}$$

Substituting $\lambda(\tau_2)$ into the left-hand side of $\mathfrak{G} = 0$ and taking the derivative with respect to τ_2, we have

$$\left(\frac{\mathrm{d}\lambda}{\mathrm{d}\tau_2}\right)^{-1} = \frac{\frac{\mu\sigma+\rho-\delta\mu}{\mu\sigma+\rho} - \left(2\lambda - \frac{\rho\delta\mu}{(\mu\sigma+\rho)^2}\right)e^{\lambda\tau_2}}{\frac{\mu\sigma+\rho-\delta\mu}{\mu\sigma+\rho}(\lambda-\rho)\lambda} - \frac{\tau_2}{\lambda}, \tag{3.6}$$

which leads to

$$\begin{aligned} \Re\left[\left(\frac{\mathrm{d}\lambda}{\mathrm{d}\tau_2}\right)^{-1}\right]_{\lambda=i\omega_0} &= \Re\left[\frac{1}{(\lambda-\rho)\lambda}\right]_{\lambda=i\omega_0} - \Re\left[\frac{\left(2\lambda - \frac{\rho\delta\mu}{(\mu\sigma+\rho)^2}\right)e^{\lambda\tau_2}}{\frac{\mu\sigma+\rho-\delta\mu}{\mu\sigma+\rho}(\lambda-\rho)\lambda}\right]_{\lambda=i\omega_0} \\ &= \frac{2\omega_0^2 + \frac{\rho^2\delta^2\mu^2}{(\mu\sigma+\rho)^4} - \left(\frac{\mu\sigma+\rho-\delta\mu}{\mu\sigma+\rho}\right)^2}{(\omega_0^2+\rho^2)\left(\frac{\mu\sigma+\rho-\delta\mu}{\mu\sigma+\rho}\right)^2} = \frac{\sqrt{\Delta_1}}{(\omega_0^2+\rho^2)\left(\frac{\mu\sigma+\rho-\delta\mu}{\mu\sigma+\rho}\right)^2} > 0. \end{aligned}$$

This suggests that the root crosses the imaginary axis from left to right at $\tau_2 = \tau_{2_0}$, indicating that E_1 becomes unstable.

(ii) The characteristic equation of system (2.3) at E_2 is

$$\left(\lambda - \frac{\varepsilon\sigma + \beta\rho\sigma - \varepsilon\delta}{\varepsilon\sigma}\right)(\lambda^2 + (\alpha\lambda + \rho\alpha)e^{-\lambda\tau_1}) = 0. \tag{3.7}$$

Obviously, $\frac{\varepsilon\sigma+\beta\rho\sigma-\varepsilon\delta}{\varepsilon\sigma}$ is a characteristic root of Eq (3.7), which is positive if $\varepsilon\sigma+\beta\rho\sigma-\varepsilon\delta > 0$, indicating that E_2 is unstable. If $\varepsilon\sigma + \beta\rho\sigma - \varepsilon\delta < 0$, we only need to consider $\mathfrak{T}(\lambda) := \lambda^2 + (\alpha\lambda + \rho\alpha)e^{-\lambda\tau_1} = 0$. Assume that $\lambda = i\xi(\xi > 0)$ is a root of $\mathfrak{T}(\lambda) = 0$. Then we have

$$\begin{cases} \alpha\rho\cos(\xi\tau_1) + \alpha\xi\sin(\xi\tau_1) = \xi^2, \\ \alpha\xi\cos(\xi\tau_1) - \alpha\rho\sin(\xi\tau_1) = 0, \end{cases} \tag{3.8}$$

which leads to

$$\xi^4 - \alpha^2\xi^2 - \alpha^2\rho^2 = 0. \tag{3.9}$$

Because $-\alpha^2\rho^2 < 0$, Equation (3.9) has a unique positive root $\xi_0^2 = \frac{\alpha^2+\sqrt{\Delta_2}}{2}, \Delta_2 = \alpha^4 + 4\alpha^2\rho^2$. Substituting ξ_0^2 into Eq (3.8), we obtain

$$\tau_{1_n} = \frac{1}{\xi_0}\left\{\arccos\frac{\rho\xi_0^2}{\alpha(\rho^2 + \xi_0^2)} + 2n\pi\right\}, n = 0, 1, 2, \ldots \tag{3.10}$$

Moreover, we can compute from $\mathfrak{T}(\lambda) = 0$ that

$$\left(\frac{\mathrm{d}\lambda}{\mathrm{d}\tau_1}\right)^{-1} = \frac{2\lambda e^{\lambda\tau_1} + \alpha}{(\alpha\lambda + \rho\alpha)\lambda} - \frac{\tau_1}{\lambda}, \tag{3.11}$$

which leads to

$$\begin{aligned} \mathfrak{R}\left[\left(\frac{\mathrm{d}\lambda}{\mathrm{d}\tau_1}\right)^{-1}_{\lambda=i\xi_0}\right] &= \frac{2\alpha\xi_0^2(\rho\cos(\xi_0\tau_1) + \xi_0\sin(\xi_0\tau_1)) + \alpha^2\xi_0^2}{\alpha^2\xi_0^4 - \rho^2\alpha^2\xi_0^2} \\ &= \frac{2\xi_0^2 - \alpha^2}{\alpha^2\xi_0^2 + \rho^2\alpha^2} = \frac{\sqrt{\Delta_2}}{\alpha^2\xi_0^2 + \rho^2\alpha^2} > 0. \end{aligned}$$

This suggests that the root crosses the imaginary axis from left to right at $\tau_1 = \tau_{1_0}$, indicating that E_2 becomes unstable. □

Next, let us delve into the local stability of $E^*(x^*, y^*, z^*)$ and explore the possible Hopf bifurcations at E^*. E^* satisfies the equation

$$\begin{cases} \alpha\left(1 - \frac{x^*}{z^*}\right) - y^* = 0, \\ \left(1 - \frac{y^*}{z^*}\right) + \beta x^* - \frac{\delta}{\sigma + y^*} = 0, \\ \rho - \varepsilon x^* - \mu y^* = 0. \end{cases} \tag{3.12}$$

To simplify the analysis, let $\bar{x}(t) = x(t) - x^*, \bar{y}(t) = y(t) - y^*, \bar{z}(t) = z(t) - z^*$, and still denote $x(t), y(t), z(t)$, respectively. The linearized part of the system (2.3) at $E^*(x^*, y^*, z^*)$ is

$$\begin{cases} \dfrac{\mathrm{d}x}{\mathrm{d}t} = -x^* y(t) - \dfrac{\alpha x^*}{z^*} x(t-\tau_1) + \dfrac{\alpha x^{*2}}{z^{*2}} z(t-\tau_1), \\ \dfrac{\mathrm{d}y}{\mathrm{d}t} = \beta y^* x(t) + \dfrac{\delta y^*}{(\sigma + y^*)^2} y(t) - \dfrac{y^*}{z^*} y(t-\tau_2) + \dfrac{y^{*2}}{z^{*2}} z(t-\tau_2), \\ \dfrac{\mathrm{d}z}{\mathrm{d}t} = -\varepsilon z^* x(t) - \mu z^* y(t). \end{cases} \tag{3.13}$$

Therefore, the corresponding characteristic equation of system (3.13) is given by:

$$\lambda^3 + m_2\lambda^2 + m_1\lambda + (b_2\lambda^2 + b_1\lambda + b_0)e^{-\lambda\tau_1} + (c_2\lambda^2 + c_1\lambda + c_0)e^{-\lambda\tau_2} + (d_1\lambda + d_0)e^{-\lambda(\tau_1+\tau_2)} = 0, \tag{3.14}$$

where

$$m_2 = -\frac{\delta y^*}{(\sigma + y^*)^2}, m_1 = \beta x^* y^*, b_2 = \frac{\alpha x^*}{z^*}, b_1 = \frac{\varepsilon\alpha x^{*2}}{z^*} - \frac{\alpha\delta x^* y^*}{(\sigma + y^*)^2 z^*}, b_0 = \frac{\alpha\beta\mu x^{*2} y^*}{z^*} - \frac{\alpha\delta\varepsilon x^{*2} y^*}{(\sigma + y^*)^2 z^*},$$
$$c_2 = \frac{y^*}{z^*}, c_1 = \frac{\mu y^{*2}}{z^*}, c_0 = \frac{-\varepsilon x^* y^{*2}}{z^*}, d_1 = \frac{\alpha x^* y^*}{z^{*2}}, \text{and } d_0 = \frac{\alpha\varepsilon x^{*2} y^* + \mu\alpha x^* y^{*2}}{z^{*2}}.$$

In the following, we apply the method used in Ruan and Wei [39] to investigate the distribution of roots of the transcendental equation (3.14). As system (2.3) has two time delays, τ_1 and τ_2, we consider the following four cases.

Case 1: $\tau_1 = \tau_2 = 0$.

The characteristic equation (3.14) becomes:

$$\lambda^3 + m_{12}\lambda^2 + m_{11}\lambda + m_{10} = 0, \tag{3.15}$$

where

$$m_{10} = \frac{\alpha\beta\mu x^{*2} y^*}{z^*} + \frac{\alpha\varepsilon x^{*2} y^* + \mu\alpha x^* y^{*2}}{z^{*2}} - \frac{\alpha\delta x^* y^*}{(\sigma + y^*)^2 z^*} - \frac{\varepsilon x^* y^{*2}}{z^*},$$
$$m_{11} = x^*\beta y^* + \frac{\alpha x^*}{z^*} + \frac{\mu y^{*2}}{z^*} + \frac{\varepsilon\alpha x^{*2}}{z^*} - \frac{\alpha\delta x^* y^*}{(\sigma + y^*)^2 z^*}, \; m_{12} = \frac{\alpha x^*}{z^*} + \frac{y^*}{z^*} - \frac{\delta y^*}{(\sigma + y^*)^2}.$$

By Routh-Hurwitz criterion, we can conclude that all of the roots of Eq (3.15) have negative real parts if and only if

(H1) $m_{12} > 0, m_{10} > 0, \; m_{11}m_{12} > m_{10}$

are satisfied. Namely, when $\tau_1 = \tau_2 = 0$, the coexistence equilibrium E^* is locally asymptotically stable provided **(H1)** is satisfied.

Case 2: $\tau_1 > 0, \; \tau_2 = 0$.

The characteristic equation (3.14) becomes:

$$\lambda^3 + m_{22}\lambda^2 + m_{21}\lambda + m_{20} + (b_{22}\lambda^2 + b_{21}\lambda + b_{20})e^{-\lambda\tau_1} = 0, \tag{3.16}$$

where

$$m_{22} = m_2 + c_2,\ m_{21} = m_1 + c_1,\ m_{20} = c_0,\ b_{22} = b_2,\ b_{21} = b_1 + d_1, \text{and } b_{20} = b_0 + d_0.$$

Assume that $\lambda = i\omega_1(\omega_1 > 0)$ is a root of Eq (3.16). By separating the real part and imaginary part, we obtain

$$\begin{cases} (b_{20} - b_{22}\omega_1^2)\cos(\omega_1\tau_1) + b_{21}\omega_1 \sin(\omega_1\tau_1) = m_{22}\omega_1^2 - m_{20}, \\ b_{21}\omega_1 \cos(\omega_1\tau_1) + (b_{22}\omega_1^2 - b_{20})\sin(\omega_1\tau_1) = \omega_1^3 - m_{21}\omega_1, \end{cases} \tag{3.17}$$

which yields

$$\omega_1^6 + e_{22}\omega_1^4 + e_{21}\omega_1^2 + e_{20} = 0, \tag{3.18}$$

where

$$e_{22} = m_{20}^2 - b_{20}^2,\ e_{21} = m_{21}^2 - b_{21}^2 - 2m_{20}m_{22} + 2b_{20}b_{22}, \text{ and } e_{20} = m_{22}^2 - b_{22}^2 - 2m_{21}.$$

Let $\omega_1^2 = x$. Then Eq (3.18) becomes

$$h(x) := x^3 + e_{22}x^2 + e_{21}x + e_{20} = 0. \tag{3.19}$$

We need only study the existence and number of positive roots for Eq (3.19). We can compute that

$$\frac{\mathrm{d}h(x)}{\mathrm{d}x} = 3x^2 + 2e_{22}x + e_{21}. \tag{3.20}$$

If $\triangle = e_{22}^2 - 3e_{21} \leq 0$, we have $\frac{\mathrm{d}h(x)}{\mathrm{d}x} \geq 0$, and thus $h(x)$ monotonically increases for $x \in [0, +\infty)$. If $\triangle > 0$, Equation (3.20) has two different real roots:

$$x_1{}^* = \frac{-e_{22} + \sqrt{e_{22}^2 - 3e_{21}}}{3},\ x_2{}^* = \frac{-e_{22} - \sqrt{e_{22}^2 - 3e_{21}}}{3}. \tag{3.21}$$

Obviously, $x_2^* < x_1^*$, and x_2^* and x_1^* are respectively the local maximum point and local minimum point. Notice the geometric characteristics of the cubic polynomial equation and also that $h(0) = e_{20}$ and $\lim\limits_{x\to+\infty} h(x) = +\infty$. We can make clear the number and existence of positive roots of Eq (3.19). The detailed analyses are provided in Appendix A. Without loss of generality, we assume the conditions in **(H2)** hold, that is,

(H2) $e_{20} < 0$, $\Delta > 0$ and $x_2^* > 0$; $h(x_2^*) > 0$ and $h(x_1^*) < 0$.

In this situation, Equation (3.18) has three positive roots denoted respectively by $\omega_{1,i}, i = 1, 2, 3$ ($\omega_{1,1} < \omega_{1,2} < \omega_{1,3}$). It then follows from Eq (3.17) that

$$\cos(\omega_1\tau_1) = \frac{(m_{22}\omega_1^2 - m_{20})(b_{20} - b_{22}\omega_1^2) + b_{21}\omega_1(\omega_1^3 - m_{21}\omega_1)}{(b_{20} - b_{22}\omega_1^2)^2 + b_{21}^2\omega_1^2}, \tag{3.22}$$

from which we obtain that

$$\tau_{1,i}^{(\kappa)} = \frac{1}{\omega_{1,i}} \arccos\left[\frac{(m_{22}\omega_{1,i}^2 - m_{20})(b_{20} - b_{22}\omega_{1,i}^2) + b_{21}\omega_{1,i}(\omega_{1,i}^3 - m_{21}\omega_{1,i})}{(b_{20} - b_{22}\omega_{1,i}^2)^2 + b_{21}^2\omega_{1,i}^2}\right] + \frac{2\kappa\pi}{\omega_{1,i}} \tag{3.23}$$

for $\kappa = 0, 1, 2, \cdots; i = 1, 2, 3$.

Now we verify that the transversality condition holds. Differentiating both sides of Eq (3.16) with respect to τ_1, we can obtain

$$\left(\frac{\mathrm{d}\lambda}{\mathrm{d}\tau_1}\right)^{-1} = \frac{3\lambda^2 + 2m_{22}\lambda + m_{21}}{-\lambda(\lambda^3 + m_{22}\lambda^2 + m_{21}\lambda + m_{20})} + \frac{2b_{22}\lambda + b_{21}}{\lambda(b_{22}\lambda^2 + b_{21}\lambda + b_{20})} - \frac{\tau_1}{\lambda}. \tag{3.24}$$

Through some sophisticated calculations, we get

$$\Re\left\{\frac{\mathrm{d}(\lambda)}{\mathrm{d}\tau_1}\right\}^{-1}_{\lambda=i\omega_1} = \frac{h'(\omega_1^2)}{b_{21}^2\omega_1^2 + (b_{20} - b_{22}\omega_1^2)^2}. \tag{3.25}$$

Lemma 3.2. *Assume the conditions in **(H2)** hold. Then*

$$sign\left\{\frac{\mathrm{d}(\Re\lambda)}{\mathrm{d}\tau_1}\right\}_{\lambda=i\omega_{1,1}} = signh'(\omega_{1,1}^2) > 0,$$

$$sign\left\{\frac{\mathrm{d}(\Re\lambda)}{\mathrm{d}\tau_1}\right\}_{\lambda=i\omega_{1,2}} = signh'(\omega_{1,2}^2) < 0,$$

$$sign\left\{\frac{\mathrm{d}(\Re\lambda)}{\mathrm{d}\tau_1}\right\}_{\lambda=i\omega_{1,3}} = signh'(\omega_{1,3}^2) > 0.$$

Proof. 1) Based on **(H2)**, we have $h(0) = e_{20} < 0$, $h(x_2^*) > 0$, and $h'(x) > 0 \in [0, x_2^*]$. By the zero existence theorem, we know that there exists a unique $\omega_{1,1}^2 \in (0, x_2^*)$, and, in addition, we have $h'(\omega_{1,1}^2) > 0$.

2) From **(H2)**, we may obtain $h(x_2^*) > 0, h(x_1^*) < 0$, and $h'(x) < 0 \in [x_2^*, x_1^*]$. By the zero existence theorem, we know that there exists a unique $\omega_{1,2}^2 \in (x_2^*, x_1^*)$, so $h'(\omega_{1,2}^2) < 0$ is verified.

3) Finally, verify the symbol at $h'(\omega_{1,3}^2)$. By the zero existence theorem, $h(x_1^*) < 0$, $\lim\limits_{x\to+\infty} h(x) = +\infty$, and $h'(x) > 0 \in [x_2^*, +\infty)$, so we know that there exists a unique $\omega_{1,3}^2 \in (x_2^*, +\infty)$, and in addition we have $h'(\omega_{1,3}^2) > 0$. □

For the case when the characteristic equation (3.16) has three pairs of conjugate complex roots, the process of analyzing stability and switching phenomena can be relatively complex. As the time delay τ_1 increases gradually and passes through the critical values of $\tau_{1,1}^{(\kappa)}$ and $\tau_{1,3}^{(\kappa)}$, the system may undergo a transition from stable to unstable, and as the time delay τ_1 passes through the critical values of $\tau_{1,2}^{(\kappa)}$, the system may be switched from unstable back to stable. Thus, stability switch phenomena may occur and the specific situations of stabilizing switches depend on the relative positions of these critical time-delay values.

For the sake of narrative convenience, we reorder all the critical values $\{\tau_{1,i}^{(\kappa)}\}$, $i = 1, 2, 3; \kappa = 0, 1, 2, \cdots$ as $\{\tau_1^{(\kappa)}\}$, $\kappa = 0, 1, 2, \cdots$ such that $0 < \tau_1^{(0)} < \tau_1^{(1)} < \tau_1^{(2)} < \cdots$, and assume that the system undergoes a stability switch from stable to unstable and then from unstable to stable, and after finite times like this, the system becomes unstable eventually. We summarize these as the following theorem.

Theorem 3.3. *For system* (2.3) *with* $\tau_1 > 0$ *and* $\tau_2 = 0$*, if* ***(H1)*** *and* ***(H2)*** *hold, then there exists a* $M \in \mathbb{N}$ *such that when* $\tau_1 \in (0, \tau_1^{(0)}) \bigcup (\tau_1^{(1)}, \tau_1^{(2)}) \bigcup \cdots \bigcup (\tau_1^{(M-1)}, \tau_1^{(M)})$*, all the roots of Eq* (3.16) *have negative real part, and thus the system of* (2.3) *is locally asympotically stable; when* $\tau_1 \in (\tau_1^{(0)}, \tau_1^{(1)}) \bigcup (\tau_1^{(2)}, \tau_1^{(3)}) \bigcup \cdots \bigcup (\tau_1^{(M)}, +\infty)$*, at least one root of Eq* (3.16) *has a positive real part, and thus the system of* (2.3) *is unstable. In addition, the model undergoes a Hopf bifurcation at* E^* *when* $\tau_1 = \tau_1^{(\kappa)}, \kappa \in \mathbb{N}$.

Case 3: $\tau_2 > 0, \tau_1 = 0$.

Analyzing similarly as in Case 2, we have the following theorem.

Theorem 3.4. *For system* (2.3) *with* $\tau_2 > 0$ *and* $\tau_1 = 0$*, the equilibrium* E^* *may undergo a finite number of stability switches, that is there is a* $N \in \mathbb{N}$ *such that it is locally asymptotically stable for* $\tau_2 \in (0, \tau_2^{(0)}) \bigcup (\tau_2^{(1)}, \tau_1^{(2)}) \bigcup \cdots \bigcup (\tau_2^{(N-1)}, \tau_2^{(N)})$*; and when* $\tau_2 \in (\tau_2^{(0)}, \tau_2^{(1)}) \bigcup (\tau_2^{(2)}, \tau_2^{(3)}) \bigcup \cdots \bigcup (\tau_2^{(N)}, +\infty)$*, the equilibrium point* E^* *is unstable. Additionally, model* (2.3) *undergoes a Hopf bifurcation at* E^* *for each* $\tau_2 = \tau_2^{(\kappa)}, \kappa \in \mathbb{N}$.

Case 4: $\tau_1 > 0, \tau_2 > 0$.

In this case, we choose τ_1 as the bifurcation parameter and τ_2 in one of its stable intervals, say $(0, \tau_2^{(0)})$ (the same below). Assume that $\lambda = i\omega_1^*(\omega_1^* > 0)$ is a characteristic root of Eq (3.14), then we can obtain

$$\begin{aligned} \mathscr{N}_1(\omega_1^*, \tau_2) &= \mathscr{K}_1(\omega_1^*, \tau_2)\cos\omega_1^*\tau_1^* - \mathscr{K}_2(\omega_1^*, \tau_2)\sin\omega_1^*\tau_1^*, \\ \mathscr{N}_2(\omega_1^*, \tau_2) &= \mathscr{K}_2(\omega_1^*, \tau_2)\cos\omega_1^*\tau_1^* + \mathscr{K}_1(\omega_1^*, \tau_2)\sin\omega_1^*\tau_1^*, \end{aligned} \tag{3.26}$$

where

$$\begin{aligned} \mathscr{K}_1(\omega_1^*, \tau_2) &= b_1\omega_1^* + d_1\omega_1^*\cos(\omega_1^*\tau_2) - d_0\sin(\omega_1^*\tau_2), \\ \mathscr{K}_2(\omega_1^*, \tau_2) &= -b_2\omega_1^{*2} + b_0 + d_1\omega_1^*\sin(\omega_1^*\tau_2) + d_0\cos(\omega_1^*\tau_2), \\ \mathscr{N}_1(\omega_1^*, \tau_2) &= \omega_1^{*3} - m_1\omega_1^* - c_1\omega_1^*\cos(\omega_1^*\tau_2) - c_2\omega_1^{*2}\sin(\omega_1^*\tau_2) + c_0\sin(\omega_1^*\tau_2), \\ \mathscr{N}_2(\omega_1^*, \tau_2) &= m_2\omega_1^{*2} + c_2\omega_1^{*2}\cos(\omega_1^*\tau_2) - c_1\omega_1^*\sin(\omega_1^*\tau 2) - c_0\cos(\omega_1^*\tau_2). \end{aligned}$$

Then, adding the squares of the above two equations, we obtain

$$G_1(\omega_1^*) + G_2(\omega_1^*)\sin(\omega_1^*\tau_2) + G_3(\omega_1^*)\cos(\omega_1^*\tau_2) = 0, \tag{3.27}$$

where

$$\begin{aligned} G_1(\omega_1^*) =& \omega_1^{*6} + (c_2^2 + m_2^2 - b_2^2 - 2m_1)\omega_1^{*4} + (m_1^2 + c_1^2 - 2c_0c_2 - b_1^2 - d_1^2 + 2b_0b_2)\omega_1^{*2} \\ &+ c_0^2 - d_0^2 - b_0^2, \\ G_2(\omega_1^*) =& -2c_2\omega_1^{*5} + (2c_0 + 2c_2m_1 - 2c_1m_2 + 2b_2d_1)\omega_1^{*3} + (2b_1d_0 - 2b_0d_1)\omega_1^*, \\ G_3(\omega_1^*) =& (-2c_1 + 2c_2m_2)\omega_1^{*4} + (2c_1m_1 - 2c_0m_2 - 2b_1d_1 + 2b_2d_0)\omega_1^{*2}. \end{aligned}$$

It is difficult to discuss the roots of Eq (3.27). To get the main conclusion, we assume that Eq (3.27) has a finite number of positive real roots $\omega_{1,i}^*(i = 1, 2, \cdots, h)$ and that for each $\omega_{1,i}^*$, there is a series of $\{\tau_{1,i}^{(\zeta)} | i = 1, 2, \cdots, h; \zeta = 0, 1, 2, \cdots\}$ satisfying Eq (3.27), where

$$\tau_{1,i}^{(\zeta)}(\tau_2) = \frac{1}{\omega_{1,i}^*}\arccos\left(\frac{\mathscr{N}_1(\omega_{1,i}^*, \tau_2)\mathscr{K}_1(\omega_1^{*(i)}, \tau_2) + \mathscr{N}_2(\omega_{1,i}^*, \tau_2)\mathscr{K}_2(\omega_{1,i}^*, \tau_2)}{\mathscr{K}_1^2(\omega_{1,i}^*, \tau_2) + \mathscr{K}_2^2(\omega_{1,i}^*, \tau_2)}\right) + \frac{2\zeta\pi}{\omega_{1,i}^*}. \tag{3.28}$$

Let $\tau_{10}^*(\tau_2) = \min\{\tau_{1,i}^{(\zeta)}(\tau_2)|\ i = 1, 2, \cdots, h; \zeta = 0, 1, 2, \cdots\}$. When $\tau_1 = \tau_{10}^*(\tau_2)$, Equation (3.28) has a pair of purely imaginary roots $i\omega_{10}^*$ for τ_2 in its stable intervals. Of course, we should verify the transversality condition. Taking the derivative on both sides of Eq (3.14) with respect to τ_1 and substituting $\lambda = i\omega_{10}^*$, we get

$$\Re\left(\frac{\mathrm{d}\lambda}{\mathrm{d}\tau_1}\right)^{-1}_{\lambda=i\omega_{10}^*} = \Re\left(\frac{R_1 + iM_1}{R_2 + iM_2}\right)^{-1}_{\lambda=i\omega_{10}^*} = \frac{R_1R_2 + M_1M_2}{R_2^2 + M_2^2}, \tag{3.29}$$

where

$$\begin{aligned}
R_1 =&(-3\omega_{10}^{*2} + m_1)\cos(\omega_{10}^*\tau_{10}^*) - 2m_2\omega_{10}^*\sin(\omega_{10}^*\tau_{10}^*) + (c_2\tau_2\omega_{10}^{*2} - c_0\tau_2 + c_1)\cos(\omega_{10}^*(\tau_{10}^* - \tau_2))\\
&+ (c_1\omega_{10}^*\tau_2 - 2c_2\omega_{10}^*)\sin(\omega_{10}^*(\tau_{10}^* - \tau_2)) + (d_1 - d_0\tau_{10}^*)\cos(\omega_{10}^*\tau_2) - d_1\omega_{10}^*\tau_{10}^*\sin(\omega_{10}^*\tau_2) + b_1,\\
M_1 =&2m_2\omega_{10}^*\cos(\omega_{10}^*\tau_{10}^*) + (-3\omega_{10}^{*2} + m_1)\sin(\omega_{10}^*\tau_{10}^*)(2c_2\omega_{10}^* - c_1\omega_{10}^*\tau_2)\cos(\omega_{10}^*(\tau_{10}^* - \tau_2))\\
&+ (\omega_{10}^{*2}c_2\tau_2 - c_0\tau_2 + c_1)\sin(\omega_{10}^*(\tau_{10}^* - \tau_2)) - d_1\omega_{10}^*\cos(\omega_{10}^*\tau_2) + (\tau_{10}^*d_0 - d_1)\sin(\omega_{10}^*\tau_2) + 2b_2\omega_{10}^*,\\
R_2 =&-b_1\omega_{10}^{*2} - d_1\omega_{10}^{*2}\cos(\omega_{10}^*\tau_2) + d_0\omega_{10}^*\sin(\omega_{10}^*\tau_2),\\
M_2 =&-b_2\omega_{10}^{*3} + b_0\omega_{10}^* + d_1\omega_{10}^{*2}\sin(\omega_{10}^*\tau_2) + d_0\omega_{10}^*\cos(\omega_{10}^*\tau_2).
\end{aligned}$$

We make the following hypothesis:

(H3) $sign\left\{\left[\frac{\mathrm{d}(\Re\lambda)}{(\mathrm{d}\tau_1)}\right]^{-1}\right\}_{\lambda=i\omega_{10}^*} = R_1R_2 + M_1M_2 \neq 0.$

Using the same logic as above, model (2.3) can exhibit the phenomenon of stability switches. For convenience, here we assume that once E^* loses its stability, it will be unstable forever. Then we will see the following results.

Theorem 3.5. *For model* (2.3) *with* $\tau_1 > 0$ *and* τ_2 *in its stable intervals, if* ***(H1)*** *and* ***(H3)*** *hold, then the equilibrium* E^* *is asymptotically stable when* $\tau_1 \in (0, \tau_{10}^*(\tau_2))$ *and unstable for* $\tau_1 \in (\tau_{10}^*(\tau_2), +\infty)$. *Moreover, model* (2.3) *undergoes a Hopf bifurcation at the equilibrium* E^* *for each* $\tau_1 = \tau_{10}^*(\tau_2)$.

4. Direction and stability of the Hopf bifurcation

In this section, we shall discuss the direction and stability of the Hopf bifurcation periodic solution of system (2.3) with respect to τ_1 and $\tau_2 \in [0, \tau_2^{(0)})$. Using the normal method of Hassard [40] and the center manifold theory, for $\tau_2 \in [0, \tau_2^{(0)})$, we derive explicit formulas to determine the properties of the Hopf bifurcation at the critical value $\tau_1 = \tau_{10}^*$. For the readability of the article, we defer the detailed derivation to Appendix B.

Using Hassard's method [40], we can calculate g_{21} and compute the following values determining the qualitative behavior of the bifurcating periodic solutions at $\tau = \tau_{10}^*$:

$$\begin{aligned}
c_1(0) &= \frac{i}{2\tau_{10}^*\omega_{10}^*}\left(g_{11}g_{20} - |2g_{11}|^2 - \frac{|g_{02}|^2}{3}\right) + \frac{g_{21}}{2},\\
\mu_2 &= -\frac{\Re\{c_1(0)\}}{\Re\{\lambda'(\tau_{10}^*)\}},\\
\beta_2 &= 2\Re\{c_1(0)\},\\
T_2 &= -\frac{\Im\{c_1(0)\} + \mu_2\Im\{\lambda'(\tau_{10}^*)\}}{\tau_{10}^*\omega_{10}^*},
\end{aligned} \tag{4.1}$$

where μ_2 determines the direction of the Hopf bifurcation: if $\mu_2 > 0$ ($\mu_2 < 0$), then the Hopf bifurcation is supercritical (subcritical). The stability of the bifurcating periodic solutions is determined by the sign of β_2: if $\beta_2 < 0$ ($\beta_2 > 0$), the bifurcating periodic solutions are stable (unstable). The period of the bifurcating periodic solutions is determined by the sign of T_2: if $T_2 > 0$ ($T_2 < 0$), the bifurcating periodic solutions increase (decrease).

5. Numerical examples and simulations

Based on the results of the stability analysis and bifurcation discussed in Sections 2 and 3, we will conduct numerical simulations to examine the impact of time delays on the stability and periodic solutions of system (2.3). These simulations will allow us to observe the effect of delay on the behavior of the system and the effect of changes in harvest rate on latency. By studying these aspects, we can better understand the dynamics of the system in different situations [41, 42].

Let the parameters of system (2.3) be $\alpha = 0.7$, $\beta = 0.08$, $\delta = 0.215$, $\sigma = 0.2$, $\rho = 1.165$, $\varepsilon = 0.75$, and $\mu = 3.55$. (If more data details are required, please refer to [27]), then we can get the following prey-free equilibrium $E_1 = (0, 0.32817, 0.55347)$, predator-free equilibrium $E_2 = (1.6643, 0, 1.6643)$ and the coexistence equilibrium $E^*= (0.293, 0.2704, 0.4774)$. By Theorem 3.1, because $\alpha - \frac{\rho}{\mu} \approx 0.3718 > 0$, and $\varepsilon\sigma + \beta\rho\sigma - \varepsilon\delta \approx 0.0074 > 0$, we know prey-free E_1 and predator-free E_2 are unstable. For $\tau_1 = 0, \tau_2 = 0$, under the above parameters, we can check that the conditions in **(H1)** are satisfied, and therefore the coexistence equilibrium E^* of system (2.3) is asymptotically stable (see Figure 1).

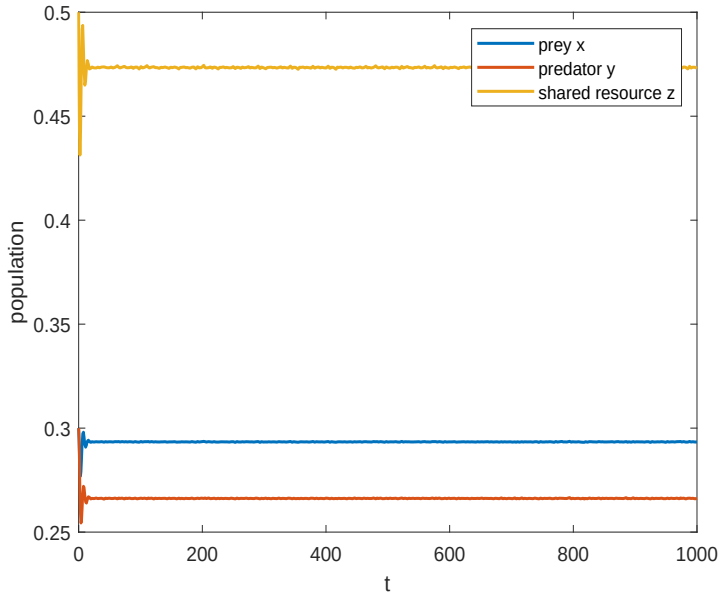

Figure 1. When $\tau_1 = \tau_2 = 0$, $E^*= (0.293, 0.2704, 0.4774)$ is asymptotically stable.

When the time delay τ_1 is within the range $[0, \tau_1^{(0)})$, the coexistence equilibrium E^* is still asymptotically stable (see Figure 2) . However, once τ_1 surpasses the critical value $\tau_1^{(0)} = 2.7415$ (at this point $\omega_{1,1} = 0.5618$), the coexistence equilibrium E^* becomes unstable, leading to a Hopf bifurcation. This bifurcation results in the emergence of a family of periodic solutions originating

from the coexistence equilibrium E^*. In summary, the stability of E^* changes at $\tau_1^{(0)}$, and this change triggers the appearance of periodic solutions (see Figure 3).

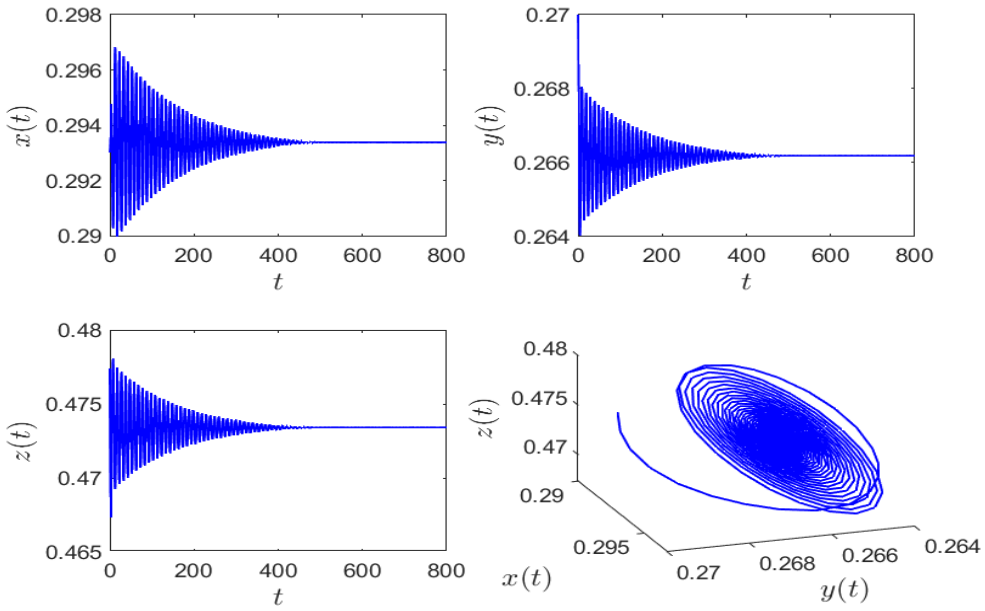

Figure 2. When $\tau_2 = 0$, E^* is asymptotically stable for $\tau_1 = 2.6 < \tau_1^{(0)} = 2.7415$.

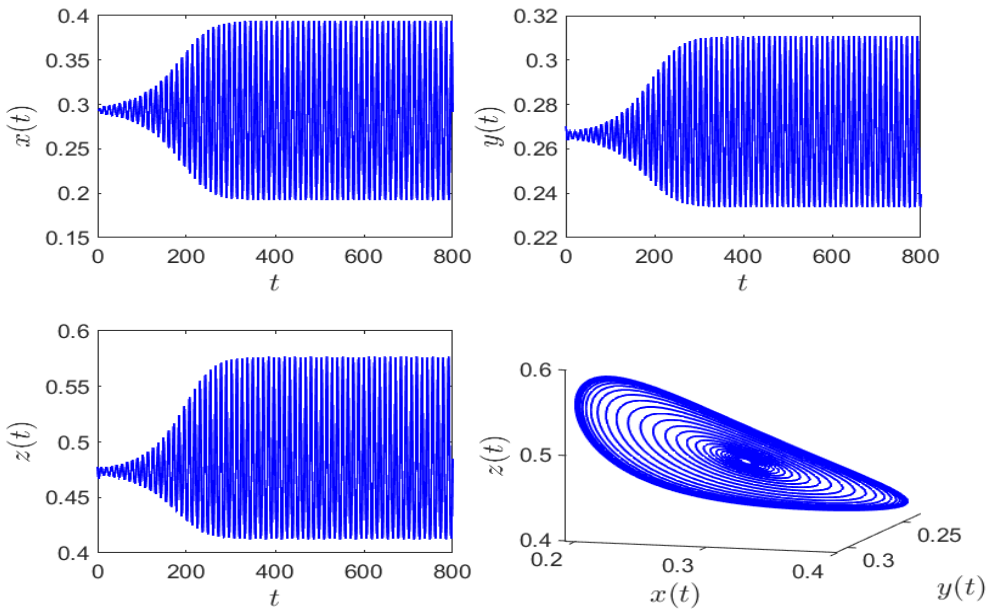

Figure 3. When $\tau_2 = 0$, E^* undergoes a Hopf bifurcation for $\tau_2 = 0, \tau_1 = 2.9 > \tau_1^{(0)} = 2.7415$.

Similarly, we have $\omega_{1,2} = 0.8895, \tau_2^{(0)} = 0.5856$, and the corresponding figures are Figures 4 and 5.

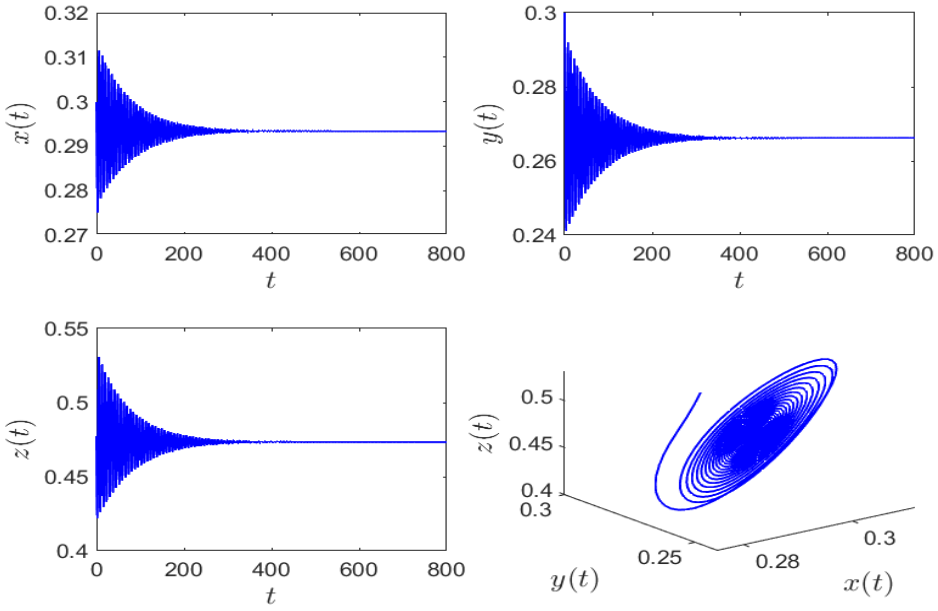

Figure 4. When $\tau_1 = 0$, E^* is asymptotically stable for $\tau_2 = 0.53 < \tau_2^{(0)} = 0.58$.

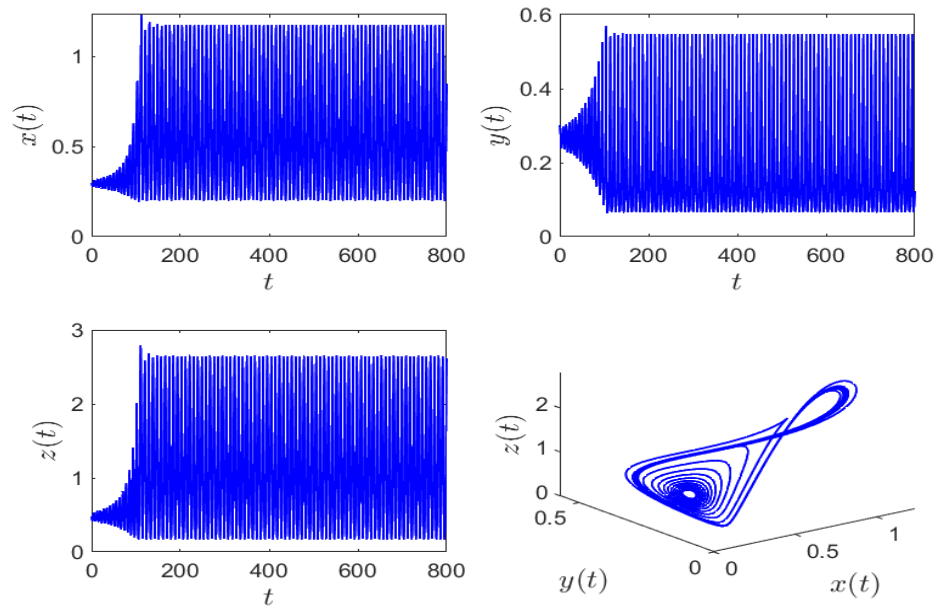

Figure 5. When $\tau_1 = 0$, E^* undergoes a Hopf bifurcation for $\tau_2 = 0.59 > \tau_2^{(0)} = 0.58$.

For $\tau_1 > 0, \tau_2 = 0.2 \in (0, \tau_2^{(0)})$, we have $\omega_{10}^* = 0.1269, \tau_{10}^* = 0.2885$. According to Theorem 3.5, E^* is asymptotically stable when $\tau_1 \in [0, 0.2885)$ (see Figure 6) and unstable when $\tau_1 > \tau_{10}^*$. After the computation of formula (4.1), we can obtain $c_1(0) = -0.2225 + 1.3699i, \beta_2 = -0.4449 < 0$, $\mu_2 = 3.2038 > 0$, and $T_2 = -0.5009 < 0$. The Hopf bifurcation is characterized as a supercritical bifurcation, where the periodic solutions are stable. This can be visually represented in Figure 7.

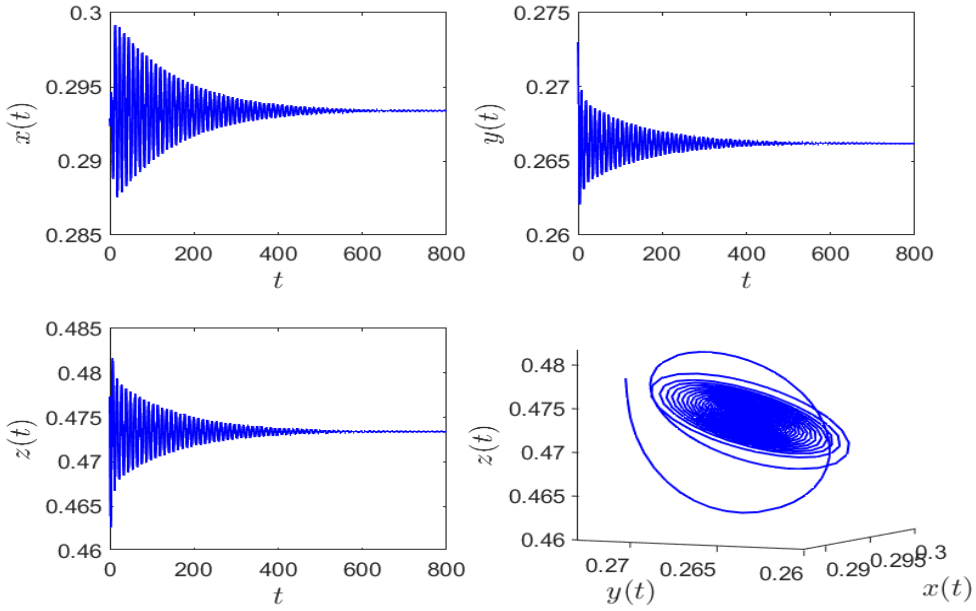

Figure 6. E^* is asymptotically stable for $\tau_1 = 2.8 < \tau_{10}^* = 2.89$ and $\tau_2 = 0.2$.

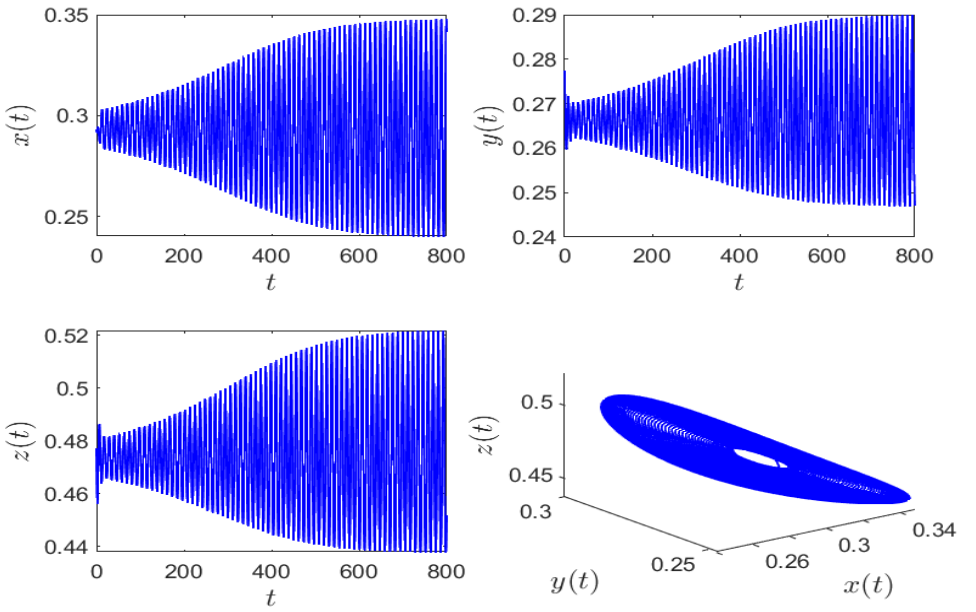

Figure 7. E^* undergoes a Hopf bifurcation for $\tau_1 = 2.9 > \tau_{10}^* = 2.89$ and $\tau_2 = 0.2$.

For an intraguild predator-prey fishery model, a stable positive equilibrium indicates a balance among the prey, predators, and the resource they are competing for. This essentially means the fishery resources are being used in a sustainable way. On the flip side, when the positive equilibrium E^* loses its stability, it will lead to an emergence of a stable periodic solution.

Next, we consider the effect of the predator harvest parameter δ on the dynamics of the system. We

can see from Figure 8 that the predator harvest parameter δ can have a significant effect on the sizes of two species and the quantity of resources, and meanwhile it can also affect the critical values of two delays: as δ increases, x^* and z^* increase, and y^* decreases, suggesting that the degree of depredation by the predator changes the numbers of predators and prey. Keeping $\tau_2 = 0.2$ constant, the higher the degree of predator capture, the smaller the corresponding τ_1 critical value τ_{10}^* will be, indicating that the degree of capture destabilizes the corresponding system (2.3).

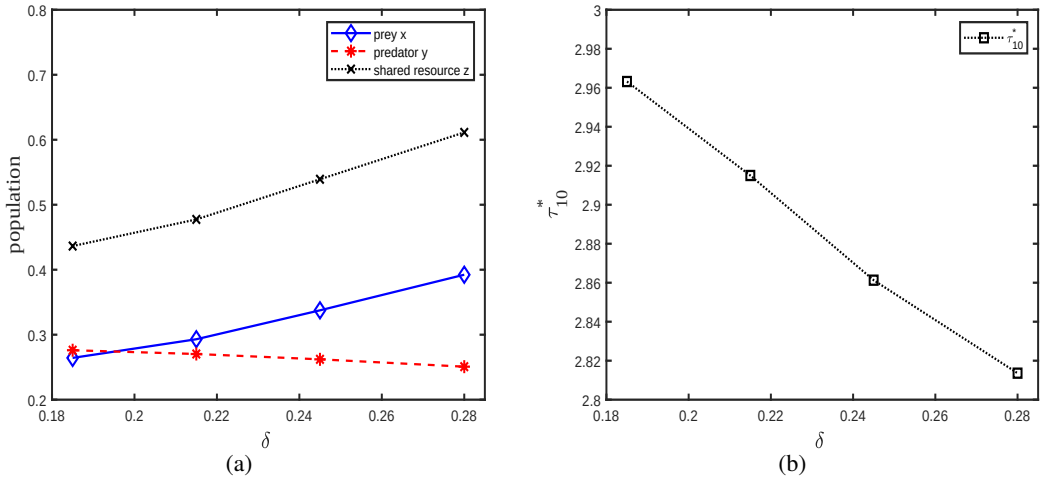

Figure 8. (a) The relationship between populations and predator harvest δ, (b) The relationship between τ_{10}^* and predator harvest δ.

6. Conclusions

In this paper, we have explored an intraguild prey-predator model (2.3) featuring two delays and a Michaelis-Menten-type harvesting. First, we analyzed the corresponding characteristic equation and discussed the stability of the prey-free equilibrium E_1 and the predator-free equilibrium E_2. According to the Hopf bifurcation theorem, we investigated the conditions for equilibrium stability and the existence of Hopf bifurcations. We employed the normal form theory and the center manifold theorem and obtained some explicit results. Specifically, when $\tau_2 \in [0, \tau_2^{(0)})$, we explored the stability and direction of Hopf bifurcations for varying values of τ_1. Finally, we validated our theoretical findings through numerical simulations.

In ecological systems, the predator, the prey, and the shared resources are expected to persist within a given set of parameters. The local bifurcation observed in such systems has ecological significance. This means that changes in the parameters can result in ecologically relevant shifts in the population dynamics of the predator and prey, along with their interactions with shared resources. In addition, when both delays surpass their critical values, they can have a significant impact on the stability of the system and cause various changes in its properties and behaviors. An increase in predator harvesting parameter δ may lead to unstable behaviors and phenomena that will influence the efficient use of shared resources by prey and predators, even if the number of predators has decreased.

To maintain sustainable fishing practices without depleting resources or driving predator species to extinction, it is crucial to employ qualitative analysis and numerical simulations in research. These methods provide insights into the dynamic behavior of ecosystems, enabling us to set limits and strike

a balance. In essence, they help determine the level of fishing that is sustainable without harming the ecosystem. Overfishing can disrupt marine ecosystems, so selecting an appropriate value for δ to achieve a balance between resource sustainability and maximizing benefits in the presence of time delays is a critical concern, which we leave for future research to address.

Use of AI tools declaration

The authors declare they have not used Artificial Intelligence (AI) tools in the creation of this article.

Acknowledgments

The authors would like to thank the National Natural Science Foundation of China (11671260; 12071293) for supporting this work.

Conflict of interest

The authors announce that there are no conflicts of interest. Sanling Yuan and Tonghua Zhang are the editorial board members for Mathematical Biosciences and Engineering and were not involved in the editorial review or the decision to publish this article.

References

1. A. J. Lotka, *Elements of Physical Biology*, Williams & Wilkins, 1925. https://doi.org/10.1038/116461b0
2. V. Volterra, Variations and fluctuations of the number of individuals in animal species living together, *ICES. J. Mar. Sci.*, **3** (1928), 3–51. https://doi.org/10.1093/icesjms/3.1.3
3. N. Bacaër, *A Short History of Mathematical Population Dynamics*, Springer, **618** (2011). https://doi.org/10.1007/978-0-85729-115-8
4. J. A. Rosenheim, H. K. Kaya, L. E. Ehler, B. A. Jaffee, Intraguild predation among biological−control agents: theory and evidence, *Biol. Control*, **5** (1995), 303–335. https://doi.org/10.1006/bcon.1995.1038
5. J. M. Fedriani, T. K. Fuller, R. M. Sauvajot, E. C. York, Competition and intraguild predation among three sympatric carnivores, *Oecologia*, **125** (2000), 258–270. https://doi.org/10.1007/s004420000448
6. E. T. Borer, C. J. Briggs, W. W. Murdoch, S. L. Swarbrick, Testing intraguild predation theory in a field system: does numerical dominance shift along a gradient of productivity?, *Ecol. Lett.*, **6** (2003), 929–935. https://doi.org/10.1046/j.1461-0248.2003.00515.x
7. G. A. Polis, C. A. Myers, R. D. Holt, The ecology and evolution of intraguild predation: potential competitors that eat each other, *Annu. Rev. Ecol. S.*, **20** (1989), 297–330. https://doi.org/10.1146/annurev.es.20.110189.001501
8. G. A. Polis, R. D. Holt, Intraguild predation: the dynamics of complex trophic interactions, *Trends Ecol. Evol.*, **7** (1992), 151–154. https://doi.org/10.1016/0169-5347(92)90208-S

9. D. R. Hart, Intraguild predation, invertebrate predators, and trophic cascades in lake food webs, *J. Theor. Biol.*, **218** (2002), 111–128. https://doi.org/10.1006/jtbi.2002.3053

10. H. V. Moeller, M. G. Neubert, M. D. Johnson, Intraguild predation enables coexistence of competing phytoplankton in a well−mixed water column, *Ecology*, **100** (2019), e02874. https://doi.org/10.1002/ecy.2874

11. H. M. Safuan, H. S. Sidhu, Z. Jovanoski, I. N. Towers, Impacts of biotic resource enrichment on a predator−prey population, *Bull. Math. Biol.*, **75** (2013), 1798–1812. https://doi.org/10.1007/s11538-013-9869-7

12. K. A. Fordjour, R. D. Parshad, M. A. Beauregard, Dynamics of a predator−prey model with generalized Holling type functional response and mutual interference, *Math. Biosci.*, **326** (2020), 108407. https://doi.org/10.1016/j.mbs.2020.108407

13. M. H. Mohd, Diversity in interaction strength promotes rich dynamical behaviours in a three−species ecological system, *Appl. Math. Comput.*, **353** (2019), 243–253. https://doi.org/10.1016/j.amc.2019.02.007

14. X. Meng, N. Qin, H. Huo, Dynamics of a food chain model with two infected predators. International Journal of Bifurcation and Chaos, *Int. J. Bifurcation Chaos*, **31** (2021). https://doi.org/10.1142/S021812742150019X

15. S. Korpinen, E. Bonsdorff, *Eutrophication and Hypoxia: Impacts of Nutrient and Organic Enrichment*, Cambridge University Press, (2015), 202–243. https://doi.org/10.1017/CBO9781139794763.008

16. X. Chen, X. Wang, Qualitative analysis and control for predator−prey delays system, *Chaos, Solitons Fractals*, **123** (2019), 361–372. https://doi.org/10.1016/j.chaos.2019.04.023

17. Y. Lv, Y. Pei, Y. Wang, Bifurcations and simulations of two predator−prey models with nonlinear harvesting, *Chaos, Solitons Fractals*, **120** (2019), 158–170. https://doi.org/10.1016/j.chaos.2018.12.038

18. S. Chakravarty, L. N. Guin, S. Ghosh, Mathematical modelling of intraguild predation and its dynamics of resource harvesting, *Int. J. Nonlinear Anal.*, **13** (2022), 837–861. https://doi.org/10.22075/ijnaa.2022.26067.3215

19. X. Wang, Y. Wang, Novel dynamics of a predator−prey system with harvesting of the predator guided by its population, *Appl. Math. Model.*, **42** (2017), 636–654. https://doi.org/10.1016/j.apm.2016.10.006

20. T. Yu, S. Yuan, Dynamic analysis of a stage−structured forest population model with non−smooth continuous threshold harvesting, *Appl. Math. Model.*, **120** (2023), 1–24. https://doi.org/10.1016/j.apm.2023.03.026

21. K. Chaudhuri, A bioeconomic model of harvesting a multispecies fishery, *Ecol. Model.*, **32** (1986), 267–279. https://doi.org/10.1016/0304-3800(86)90091-8

22. T. Das, R. N. Mukherjee, K. S. Chaudhuri, Harvesting of a prey−predator fishery in the presence of toxicity, *Appl. Math. Model.*, **33** (2009), 2282–2292. https://doi.org/10.1016/j.apm.2008.06.008

23. T. K. Ang, H. M. Safuan, Harvesting in a toxicated intraguild predator−prey fishery model with variable carrying capacity, *Chaos, Solitons Fractals*, **126** (2019), 158–168. https://doi.org/10.1016/j.chaos.2019.06.004

24. C. W. Clark, Aggregation and fishery dynamics: a theoretical study of schooling and the purse seine tuna fisheries, *Fish B-Noaa*, **77** (1979), 317–337.

25. R. P. Gupta, P. Chandra, Bifurcation analysis of modified Leslie−Gower predator−prey model with Michaelis−Menten type prey harvesting, *J. Math. Anal. Appl.*, **398** (2013), 278–295. https://doi.org/10.1016/j.jmaa.2012.08.057

26. D. Hu, H. Cao, Stability and bifurcation analysis in a predator−prey system with Michaelis−Menten type predator harvesting, *Nonlinear Anal. Real World Appl.*, **33** (2017), 58–82. https://doi.org/10.1016/j.nonrwa.2016.05.010

27. T. K. Ang, H. M. Safuan, Dynamical behaviors and optimal harvesting of an intraguild prey−predator fishery model with Michaelis−Menten type predator harvesting, *Biosystems*, **202** (2021), 104357. https://doi.org/10.1016/j.biosystems.2021.104357

28. U. S. B. U. Sharif, M. H. Mohd, Combined influences of environmental enrichment and harvesting mediate rich dynamics in an intraguild predation fishery system, *Ecol. Modell.*, **474** (2022), 110140. https://doi.org/10.1016/j.ecolmodel.2022.110140

29. Y. Shao, Global stability of a delayed predator−prey system with fear and Holling−type II functional response in deterministic and stochastic environments, *Math. Comput. Simul.*, **200** (2022), 65–77. https://doi.org/10.1016/j.matcom.2022.04.013

30. X. Wang, M. Peng, X. Liu, Stability and Hopf bifurcation analysis of a ratio−dependent predator−prey model with two time delays and Holling type III functional response, *Appl. Math. Comput.*, **268** (2015), 496–508. https://doi.org/10.1016/j.amc.2015.06.108

31. A. Kumar, B. Dubey, Modeling the effect of fear in a prey−predator system with prey refuge and gestation delay, *Int. J. Bifurcation Chaos*, **29** (2019), 1950195. https://doi.org/10.1142/S0218127419501955

32. K. Li, J. Wei, Stability and Hopf bifurcation analysis of a prey−predator system with two delays, *Chaos, Solitons Fractals*, **42** (2009), 2606–2613. https://doi.org/10.1016/j.chaos.2009.04.001

33. B. Dubey, A. Kumar, A. P. Maiti, Global stability and Hopf−bifurcation of prey−predator system with two discrete delays including habitat complexity and prey refuge, *Commun. Nonlinear Sci.*, **67** (2019), 528–554. https://doi.org/10.1016/j.cnsns.2018.07.019

34. S. Li, S. Yuan, Z. Jin, H. Wang, Bifurcation analysis in a diffusive predator−prey model with spatial memory of prey, Allee effect and maturation delay of predator, *J. Differ. Equations*, **357** (2023), 32–63. https://doi.org/10.1016/j.jde.2023.02.009

35. T. K. Kar, U. K. Pahari, Modelling and analysis of a prey−predator system with stage−structure and harvesting, *Nonlinear Anal. Real World Appl.*, **8** (2007), 601–609. https://doi.org/10.1016/j.nonrwa.2006.01.004

36. C. Xu, S. Yuan, Stability and Hopf bifurcation in a delayed predator−prey system with herd behavior, *Abstr. Appl. Anal.*, **2014** (2014), 568943. https://doi.org/10.1155/2014/568943

37. R. Shi, J. Yu, Hopf bifurcation analysis of two zooplankton−phytoplankton model with two delays, *Chaos, Solitons Fractals*, **100**, (2017), 62–73. https://doi.org/10.1016/j.chaos.2017.04.044

38. Y. Kuang, *Delay Differential Equations: with Applications in Population Dynamics*, Academic Press, 1993.

39. S. Ruan, J. Wei, On the zeros of transcendental functions with applications to stability of delay differential equations with two delays, *Math. Med. Biol.: J. IMA*, **10** (2003), 863–874. https://doi.org/10.1093/imammb/18.1.41

40. B. D. Hassard, N. D. Kazarinoff, Y. H. Wan, *Theory and Applications of Hopf Bifurcation*, Cambridge University Press, 1981. https://doi.org/10.1137/1024123

41. X. Lin, H. Wang, Stability analysis of delay differential equations with two discrete delays, *Can. Appl. Math. Q.*, **20** (2012), 519–533.

42. Q. An, E. Beretta, Y. Kuang, C. Wang, H. Wang, Geometric stability switch criteria in delay differential equations with two delays and delay dependent parameters, *J. Differ. Equations*, **266** (2019), 7073–7100. https://doi.org/10.1016/j.jde.2018.11.025

Appendix

A. Detailed analysis on the positive root distribution of Eq (3.19)

1) If $e_{20} > 0$, then we have

   (a) If $\Delta \leq 0$, then Eq (3.19) has no positive roots.

   (b) If $\Delta > 0$, then we have

   - when $x_1^* \leq 0$, then Eq (3.19) has no positive roots.
   - when $x_1^* > 0$ and $h(x_1^*) > 0$, then Eq (3.19) has no positive roots.
   - when $x_1^* > 0$ and $h(x_1^*) = 0$, then Eq (3.19) has one positive double root (i.e., x_1^*).
   - when $x_1^* > 0$ and $h(x_1^*) < 0$, then Eq (3.19) has two different positive roots.

2) If $e_{20} = 0$, then we have

   (a) If $\Delta \leq 0$, then Eq (3.19) has no positive roots.

   (b) If $\Delta > 0$, then we have

   - when $x_1^* \leq 0$, then Eq (3.19) has no positive roots.
   - when $x_2^* \leq 0 < x_1^*$, then Eq (3.19) has one positive root.
   - when $x_2^* > 0$ and $h(x_1^*) > 0$, then Eq (3.19) has no positive roots.
   - when $x_2^* > 0$ and $h(x_1^*) = 0$, then Eq (3.19) has one positive double root (i.e., x_1^*).
   - when $x_2^* > 0$ and $h(x_1^*) < 0$, then Eq (3.19) has two different positive roots.

3) If $e_{20} < 0$, then we have

   (a) If $\Delta \leq 0$, then Eq (3.19) has one positive root.

   (b) If $\Delta > 0$, then we have

- when $x_2^* \le 0$, then Eq (3.19) has one positive root.
- when $x_2^* > 0$ and $h(x_1^*)h(x_2^*) > 0$, then Eq (3.19) has one positive root.
- when $x_2^* > 0$, $h(x_2^*) = 0$ (respectively, $h(x_1^*) = 0$), then Eq (3.19) has one positive double root x_2^* (respectively, x_1^*) and one positive root.
- when $x_2^* > 0$, $h(x_2^*) > 0$ and $h(x_1^*) < 0$, then Eq (3.19) has three positive roots.

To summarize, we can have the following results on Eq (3.18).

Lemma A.1. *The following statements are true.*

1) *If one of the following four conditions holds, Equation* (3.18) *will have on positive roots.*

(i) $e_{20} \ge 0$ *and* $\Delta \le 0$*;*
(ii) $e_{20} \ge 0$, $\Delta > 0$ *and* $x_1^* \le 0$*;*
(iii) $e_{20} > 0$, $\Delta > 0$ *and* $\min\{x_1^*, h(x_1^*)\} > 0$*;*
(iv) $e_{20} = 0$, $\Delta > 0$ *and* $\min\{x_2^*, h(x_1^*)\} > 0$.

2) *If one of the following three conditions is satisfied, Equation* (3.18) *will have only one positive root.*

(i) $e_{20} = 0$, $\Delta > 0$ *and* $x_2^* \le 0 < x_1^*$.
(ii) $e_{20} < 0$, $\Delta > 0$ *and* $x_2^* \le 0$.
(iii)$e_{20} < 0$, $\Delta > 0$ *and* $\min\{x_2^*, h(x_1^*)h(x_2^*)\} > 0$.

3) *If either of the following two conditions is satisfied, Equation* (3.18) *will possess two positive roots:*

(i) $e_{20} > 0$, $\Delta > 0$ *and* $x_1^* > 0$ *and* $h(x_1^*) < 0$*;*
(ii) $e_{20} = 0$, $\Delta > 0$ *and* $x_2^* > 0$ *and* $h(x_1^*) < 0$*;*

4) *Equation* (3.18) *has three positive roots provided the following conditions hold:*

(H2) $e_{20} < 0$, $\Delta > 0$, $x_2^* > 0$, $h(x_2^*) > 0$, *and* $h(x_1^*) < 0$.

5) *Equation* (3.18) *has one double positive root provided one of the following two conditions holds:*

(i) $e_{20} > 0$, $\Delta > 0$, $x_1^* > 0$, *and* $h(x_1^*) = 0$*; (ii)* $e_{20} = 0$, $\Delta > 0$, $x_2^* > 0$, *and* $h(x_1^*) = 0$*;*

6) *Equation* (3.18) *has two positive roots (a single root and a double root) provided the following conditions hold:*

$e_{20} < 0$, $\Delta > 0$, $x_2^* > 0$, *and* $h(x_2^*) = 0$ *(or* $h(x_1^*) = 0$*).*

B. Computation of the Coefficients μ_2, β_2, and T_2

Let $\tau_1 = \tau_{10}^* + \mu, \mu \in R$, then $\mu = 0$ is the Hopf bifurcation value of the system. Let $t = s\tau_1$, $x(s\tau_1) = \widehat{x}(s)$, $y(s\tau_1) = \widehat{y}(s)$, $z(s\tau_1) = \widehat{z}(s)$, and denote $x = \widehat{x}(s)$, $y = \widehat{y}(s)$, $z = \widehat{z}(s)$, and $t = s$, then system (2.3) can be written as a functional differential equation in $C = C([-1, 0], R^3)$:

$$\dot{X}(t) = L_\mu X_t + f(\mu, X_t), \tag{B.1}$$

where $X(t) = (x(t), y(t), z(t))^T \in R^3$, $X_t(\theta) = X(t + \theta) = (x(t + \theta), y(t + \theta), z(t + \theta))^T \in C$, and $L_\mu : C \to R^3$,$F : R \times C \to R^3$ are given by

$$L_\mu(\phi) = (\tau_{10}^* + \mu)\left[A\phi(0) + B\phi(-1) + C\phi\left(-\frac{\tau_2}{\tau_{10}^*}\right)\right], \tag{B.2}$$

and

$$F(\mu,\phi) = (\tau_{10}^* + \mu)\begin{pmatrix} F_1 \\ F_2 \\ F_3 \end{pmatrix}, \tag{B.3}$$

where

$$A = \begin{pmatrix} 0 & -x^* & 0 \\ \beta y^* & \dfrac{\delta y^*}{(\sigma + y^*)^2} & 0 \\ -\varepsilon z^* & -\mu z^* & 0 \end{pmatrix}, B = \begin{pmatrix} -\dfrac{\alpha x^*}{z^*} & 0 & \dfrac{\alpha x^{*2}}{z^{*2}} \\ 0 & 0 & 0 \\ 0 & 0 & 0 \end{pmatrix}, C = \begin{pmatrix} 0 & 0 & 0 \\ 0 & -\dfrac{y^*}{z^*} & \dfrac{y^{*2}}{z^{*2}} \\ 0 & 0 & 0 \end{pmatrix},$$

$$\begin{aligned} F_1 =& h_1\phi_1(0)\phi_2(0) - h_2\phi_1(0)\phi_1(-1) + h_3\phi_1(0)\phi_3(-1) + h_3\phi_1(-1)\phi_3(-1) + h_4\phi_3^2(-1) \\ &+ h_5\phi_1(0)\phi_1(-1)\phi_3(-1) + h_6\phi_1(0)\phi_3^2(-1) + h_6\phi_1(-1)\phi_3^2(-1) + h_7\phi_3^3(-1), \\ F_2 =& k_1\phi_1(0)\phi_2(0) + k_2\phi_2^2(0) + k_3\phi_2(0)\phi_2\left(-\frac{\tau_2}{\tau_{10}^*}\right) + k_4\phi_2\left(-\frac{\tau_2}{\tau_{10}^*}\right)\phi_3\left(-\frac{\tau_2}{\tau_{10}^*}\right) \\ &+ k_4\phi_2(0)\phi_2\left(-\frac{\tau_2}{\tau_{10}^*}\right) + k_5\phi_3^2\left(-\frac{\tau_2}{\tau_{10}^*}\right) + k_6\phi_2^3(0) + k_7\phi_2(0)\phi_2\left(-\frac{\tau_2}{\tau_{10}^*}\right)\phi_3\left(-\frac{\tau_2}{\tau_{10}^*}\right) \\ &+ k_8\phi_2(0)\phi_3^2\left(-\frac{\tau_2}{\tau_{10}^*}\right) + k_8\phi_2\left(-\frac{\tau_2}{\tau_{10}^*}\right)\phi_3^2\left(-\frac{\tau_2}{\tau_{10}^*}\right) + k_9\phi_3^3\left(-\frac{\tau_2}{\tau_{10}^*}\right), \\ F_3 =& l_1\phi_2(0)\phi_3(0) + l_2\phi_1(0)\phi_3(0), \end{aligned}$$

where

$$\begin{aligned} &h_1 = -1, h_2 = -\frac{\alpha}{z^*}, h_3 = \frac{\alpha x^*}{z^{*2}}, h_4 = -\frac{\alpha x^{*2}}{z^{*3}}, h_5 = \frac{\alpha}{z^{*2}}, \\ &h_6 = -\frac{\alpha x^*}{z^{*3}}, h_7 = -\frac{\alpha x^{*2}}{z^{*4}}, k_1 = \beta, k_2 = \frac{\sigma\delta}{(\sigma + y^*)^3}, k_3 = \frac{-1}{z^*}, k_4 = \frac{y^*}{z^{*2}}, \\ &k_5 = -\frac{y^{*2}}{z^{*2}}, k_6 = -\frac{\delta\sigma}{(\sigma + y^*)^4}, k_7 = \frac{-1}{z^{*2}}, k_8 = -\frac{y^*}{z^{*3}}, k_9 = -\frac{y^{*2}}{z^{*4}}, l_1 = -\mu, l_2 = -\varepsilon. \end{aligned}$$

By the Riesz representation theorem, there exists a 3×3 matrix function $\eta(\theta,\mu)$ of bounded variatation for $\theta \in [-1, 0]$, such that

$$L_\mu\phi = \int_{-1}^{0} \mathrm{d}\eta(\theta,\mu)\phi(\theta), for\ \phi \in C. \tag{B.4}$$

In fact, we can choose

$$\eta(\theta,\mu) = (\tau_{10}^* + \mu)\left[A\delta(\theta) + B\delta(\theta+1) + C\delta\left(\theta + \frac{\tau_2}{\tau_{10}^*}\right)\right], \tag{B.5}$$

where $\delta(\theta)$ is the Dirac delta function.
For $\phi \in C([-1, 0], R^3)$, define

$$\mathscr{A}(\mu)\phi = \begin{cases} \dfrac{\mathrm{d}\phi(\theta)}{\mathrm{d}\theta}, -1 \le \theta < 0, \\ \displaystyle\int_{-1}^{0} \mathrm{d}\eta(\theta,\mu)\phi(\theta), \theta = 0, \end{cases}$$

and

$$R(\mu)\phi = \begin{cases} 0, -1 \le \theta < 0, \\ F(\mu, \phi), \theta = 0. \end{cases}$$

Then this can be transformed into the following operator equation

$$\dot{X}_t = \mathscr{A}(\mu)X_t + R(\mu)X_t, \tag{B.6}$$

which is a functional differential equation in $C([-1, 0]; R^3)$.
Denote $\mathscr{A} = \mathscr{A}(0)$,

$$\mathscr{A}^*(\mu)\phi = \begin{cases} -\dfrac{\mathrm{d}\psi(s)}{\mathrm{d}s}, 0 < s \leqslant 1, \\ \displaystyle\int_{-1}^{0} \mathrm{d}\eta^T(t, 0)\psi(-t), s = 0, \end{cases}$$

and

$$< \psi(s), \phi(\theta) >= \overline{\psi}(0)\phi(0) - \int_{-1}^{0}\int_{\xi=0}^{\theta} \overline{\psi}(\xi - \theta)\mathrm{d}\eta(\theta, 0)\psi(\xi)d\xi,$$

where $\psi \in C^*([0, 1], (R^3)^*)$. Then $\mathscr{A}^*$ are adjoint operators of $\mathscr{A}$. If $\pm i\omega_{1k}\tau_{1k}$ are eigenvalues of $\mathscr{A}$, they are eigenvalues of $\mathscr{A}^*$. Suppose that $q(\theta) = (1, q_2, q_3)^T e^{i\omega_{10}{}^*\tau_{10}{}^*\theta}$ is the eigenvector of $\mathscr{A}$ corresponding to $i\omega_{10}^*\tau_{10}^*$, that is $\mathscr{A}q(\theta) = i\omega_{10}^*\tau_{10}^* q(\theta)$. Then we can obtain that

$$\begin{aligned} q_2 &= -\frac{(\alpha\varepsilon x^{*2}z^* + \alpha x^* z^* i\omega_{10}^*)e^{-i\omega_{10}^*\tau_{10}^*} - \omega_{10}^* z^{*2}}{x^* z^{*2} i\omega_{10}^* + \alpha\mu x^{*2} z^* e^{-i\omega_{10}^*\tau_{10}^*}}, \\ q_3 &= \frac{i\omega_{10}^*(-\varepsilon x^* z^{*2} + \alpha\mu x^* z^* e^{-i\omega_{10}^*\tau_{10}^*} + i\omega_{10}^*)}{-x^* z^* \omega_{10}^{*2} + \alpha\mu x^{*2} i\omega_{10}^* e^{-i\omega_{10}^*\tau_{10}^*}}. \end{aligned}$$

Let $q^*(s) = D(1, q_2^*, q_3^*)e^{i\omega_{10}^*\tau_{10}^* s}$ be an eigenvector of $\mathscr{A}^*$corresponding to $-i\omega_{10}^*\tau_{10}^*$, then we have

$$\begin{aligned} q_2{}^* &= \frac{\omega_{10}^{*2} z^{*2} + (i\omega_{10}^* \alpha x^* z^* - \alpha\varepsilon x^{*2} z^*)e^{i\omega_{10}^*\tau_{10}^*}}{\beta y^* z^{*2} i\omega_{10}^* + \varepsilon y^{*2} z^* e^{i\omega_{10}^*\tau_2^*}}, \\ q_3{}^* &= \frac{\left(-\alpha x^* y^{*2} e^{i\omega_{10}^*\tau_{10}^*} + i\omega_{10}^*\right) e^{i\omega_{10}^*\tau_2} + \alpha\beta x^{*2} y^* z^* e^{i\omega_{10}^*\tau_{10}^*}}{\beta y^* z^{*3} i\omega_{10}^* + \varepsilon y^{*2} z^{*2} e^{i\omega_{10}^*\tau_2}}. \end{aligned}$$

For this equation, we can get

$$\begin{aligned} < q^*(s), q(\theta) > &= \overline{q}^*(0)q(0) - \int_{-1}^{0}\int_{\xi=0}^{\theta} \overline{q}^*(\xi - \theta)\mathrm{d}\eta(\theta)q(\xi)d\xi \\ &= \overline{D}(1, \overline{q}_2^*, \overline{q}_3^*)(1, q_2, q_3)^T - \overline{D}\int_{-1}^{0}\int_{\xi=0}^{\theta} (1, \overline{q}_2^*, \overline{q}_3^*)e^{i\omega_{10}^*\tau_{10}^*(\theta-\xi)}\mathrm{d}\eta(\theta)(1, q_2, q_3)^T e^{i\omega_{10}^*\tau_{10}^*\xi}d\xi \\ &= \overline{D}\left[1 + \overline{q}_2^* q_2 + \overline{q}_3^* q_3 - \int_{-1}^{0} (1, \overline{q}_2^*, \overline{q}_3^*)\theta e^{i\omega_{10}^*\tau_{10}^*\theta}\mathrm{d}\eta(\theta)(1, q_2, q_3)^T\right] \end{aligned}$$

$$= \overline{D}\left[1 + \overline{q}_2^* q_2 + \overline{q}_3^* q_3 + \tau_{10}^*\left(\frac{\alpha x^*}{z^*} - \frac{\alpha x^{*2}}{z^{*2}} q_3\right) e^{-i\omega_{10}^*\tau_{10}^*} + \tau_2\left(\frac{y^*}{z^*}\, q_2\overline{q}_2^* - \frac{y^{*2}}{z^{*2}} q_3\overline{q}_2^*\right) e^{-i\omega_{10}^*\tau_2}\right].$$

Thus, one can choose D as

$$D = \left[1 + \overline{q}_2 {q_2}^* + \overline{q}_3 q_3^* + \tau_{10}^*\left(\frac{\alpha x^*}{z^*} - \frac{\alpha x^{*2}}{z^{*2}} q_3\right) e^{i\omega_{10}^*\tau_{10}^*} + \tau_2\left(\frac{y^*}{z^*} q_2\overline{q}_2^* - \frac{y^{*2}}{z^{*2}} q_3\overline{q}_2^*\right) e^{i\omega_{10}^*\tau_2}\right]^{-1}, \tag{B.7}$$

which satisfies $< q^*(s), q(\theta) >= 1$.

In the rest of this section, applying the methods from [40] along with similar computational procedures should enable us to ascertain the coefficients for determining both the Hopf bifurcation's direction and the stability of the bifurcating periodic solutions.

$$\begin{aligned}
g_{20} =& 2\tau_{10}^*\overline{D}\Big(h_4 q_3^2 e^{-2i\omega_{10}^*\tau_{10}^*} + h_3 q_3 e^{-i\omega_{10}^*\tau_{10}^*} + h_1 q_2 + \Big((k_4 q_2 q_3 + k_5 q_3^2) e^{-2i\omega_{10}^*\tau_2} + (k_3 q_2^2 + k_4 q_2 q_3) e^{-i\omega_{10}^*\tau_2} \\
&+ k_2 q_2^2 + k_6 q_2^2 + k_1 q_2\Big)\overline{q}_2^* + (l_1 q_2 q_3 + l_2 q_3)\overline{q}_3^*\Big), \\
g_{11} =& \tau_{10}^*\overline{D}\Big(2h_4\overline{q}_3 q_3 + (h_3\overline{q}_3 + h_3 q_3) e^{-i\omega_{10}^*\tau_{10}^*} + k_4 q_2\overline{q}_3 + 2Re(h_1 q_2) + k_4\overline{q}_2 q_3 e^{-i\omega_{10}\tau_2} + (k_4 q_3\overline{q}_2 \\
&+ 2k_5 q_3\overline{q}_3 + k_3 q_2\overline{q}_2 (e^{-i\omega_{10}^*\tau_2} + e^{i\omega_{10}^*\tau_2}) + k_4 q_2\overline{q}_3 e^{i\omega_{10}^*\tau_2} + 2(k_2 + k_6) q_2\overline{q}_2 + k_1\overline{q}_2 + k_1 q_2)\overline{q}_2^* \\
&+ (l_1\overline{q}_2 q_3 + l_1 q_2\overline{q}_3 + l_2^2\overline{q}_3 q_3)\overline{q}_3^*\Big), \\
g_{02} =& 2\tau_{10}^*\overline{D}\Big(h_4\overline{q}_3^2 e^{2i\omega_{10}^*\tau_{10}^*} + h_3\overline{q}_3 e^{i\omega_{10}^*\tau_{10}^*} + h_1\overline{q}_2 + (k_4\overline{q}_2\overline{q}_3 + k_5\overline{q}_3^2) e^{2i\omega_{10}^*\tau_2} + k_3\overline{q}_2^2 e^{i\omega_{10}^*\tau_2} + k_4\overline{q}_2\overline{q}_3 e^{i\omega_{10}^*\tau_2} \\
&+ (k_2 + k_6)\overline{q}_2^2 + k_1\overline{q}_2)\overline{q}_2^* + (l_1\overline{q}_2\overline{q}_3 + l_2\overline{q}_3)\overline{q}_3^*\Big), \\
g_{21} =& \tau_{10}^*\overline{D}\Big(2h_3 q_3 W_{11}^{(1)}(0) e^{-i\omega_{10}^*\tau_{10}^*} + h_3\overline{q}_3 W_{20}^{(1)}(0) e^{i\omega_{10}^*\tau_{10}^*} h_3\overline{q}_3 W_{20}^{(1)}(-1) e^{i\omega_{10}^*\tau_{10}^*} + 2h_4\overline{q}_3 W_{20}^{(3)}\left(-\frac{\tau_2}{\tau_{10}^*}\right) e^{i\omega_{10}^*\tau_{10}^*} \\
&+ 4h_4 q_3 W_{11}^{(3)}\left(-\frac{\tau_2}{\tau_{10}^*}\right) e^{-i\omega_{10}^*\tau_{10}^*} + 2h_3 q_3 e^{-i\omega_{10}^*\tau_{10}^*} + 2h_3 q_3 W_{11}^{(1)}(-1) e^{-i\omega_{10}^*\tau_{10}^*} - 2h_2 W_{11}^{(1)}(-1) + h_1 W_{20}^{(2)}(0) \\
&- h_2 W_{20}^{(1)}(-1) + h_3 W_{20}^{(3)}\left(-\frac{\tau_2}{\tau_{10}^*}\right) + 2h_1 W_{11}^{(2)}(0) + 2h_3 W_{11}^{(3)}\left(-\frac{\tau_2}{\tau_{10}^*}\right) - 2h_2 + 2h_6 q_3^2 e^{2i\omega_{10}^*\tau_{10}^*} + 2h_1 q_2 W_{11}^{(1)}(0) \\
&+ h_1\overline{q}_2 W_{20}^{(1)}(0)\left(4h_6 q_3\overline{q}_3 + 6h_7 q_3^2\overline{q}_3 e^{-i\omega_{10}^*\tau_{10}^*}\right)\Big) + \Big(6k_9\overline{q}_3 q_3^2 e^{-i\omega_{10}^*\tau_2} + 2k_7 q_2^2\overline{q}_3 + 2k_8\overline{q}_2 q_3^2 e^{-i\omega_{10}^*\tau_2} \\
&+ 2k_7 q_2\overline{q}_2 q_3 e^{-2i\omega_{10}^*\tau_2} + k_1 W_{20}^{(2)}(0) + 2k_1 W_{11}^{(2)}(0) + k_4\overline{q}_3 W_{20}^{(2)}\left(-\frac{\tau_2}{\tau_{10}^*}\right) e^{i\omega_{10}^*\tau_2} + 4k_5 q_3 W_{11}^{(3)}\left(-\frac{\tau_2}{\tau_{10}^*}\right) e^{-i\omega_2\tau_{10}^*} \\
&+ 2k_5\overline{q}_3 W_{20}^{(3)}\left(-\frac{\tau_2}{\tau_{10}^*}\right) e^{i\omega_{10}^*\tau_2} + 2k_8\overline{q}_2 q_3^2 e^{-2i\omega_{10}^*\tau_2} + 2k_3 q_2 W_{11}^{(2)}(0) e^{i\omega_{10}^*\tau_2} + 2k_3 q_2 W_{11}^{(2)}(0) e^{-i\omega_{10}^*\tau_2} \\
&+ k_3\overline{q}_2 W_{20}^{(2)}(0) e^{i\omega_{10}^*\tau_2} + 2k_4 q_3 W_{11}^{(2)}(0) e^{-i\omega_{10}^*\tau_2} + k_4\overline{q}_3 W_{20}^{(2)}(0) e^{i\omega_{10}^*\tau_2} + 2k_4 q_2 e^{-i\omega_{10}^*\tau_2} W_{11}^{(3)}\left(-\frac{\tau_2}{\tau_{10}^*}\right) \\
&+ k_4\overline{q}_2 W_{20}^{(3)}\left(-\frac{\tau_2}{\tau_{10}^*}\right) e^{i\omega_{10}^*\tau_2} + 2k_4 q_2 W_{11}^{(2)}\left(-\frac{\tau_2}{\tau_{10}^*}\right) e^{i\omega_{10}^*\tau_2} + 2k_1 q_2 W_{11}^{(1)}(0) + 4k_2 q_2 W_{11}^{(2)}(0) + 2k_3 q_2 W_{11}^{(2)}\left(-\frac{\tau_2}{\tau_{10}^*}\right) \\
&+ 2k_4 q_2 W_{11}^{(3)}\left(-\frac{\tau_2}{\tau_{10}^*}\right) + 4k_6 q_2 W_{11}^{(2)}(0) + k_1\overline{q}_2 W_{20}^{(1)}(0) + 2k_2\overline{q}_2 W_{20}^{(2)}(0) + k_3\overline{q}_2 W_{20}^{(2)}\left(-\frac{\tau_2}{\tau_{10}^*}\right) + k_4\overline{q}_2 W_{20}^{(3)}\left(-\frac{\tau_2}{\tau_{10}^*}\right) \\
&+ 2k_6\overline{q}_2 W_{20}^{(2)}(0) + 2k_7 q_2\overline{q}_2 q_3 + 4k_8 q_2 q_3\overline{q}_3 + 4k_8 q_2 q_3\overline{q}_3 e^{-i\omega_{10}^*\tau_2}\Big)\overline{q}_2^* + \Big(l_2 W_{20}^{(3)}(0) + 2l_2 W_{11}^{(3)}(0) \\
&+ 2l_1 q_2 W_{11}^{(3)}(0) + 2l_1 q_3 W_{11}^{(2)}(0) + 2l_2 q_3 W_{11}^{(1)}(0)\overline{q}_3 + l_1\overline{q}_2 W_{20}^{(3)}(0) + l_1\overline{q}_3 W_{20}^{(2)}(0) + l_2\overline{q}_3 W_{20}^{(1)}(0)\Big)\overline{q}_3^*.
\end{aligned}$$

However,

$$W_{20}(\theta) = \frac{ig_{20}}{\omega_{10}^*\tau_{10}^*}q(0)e^{i\omega_{10}^*\tau_{10}^*\theta} + \frac{i\overline{g}_{02}}{3\omega_{10}^*\tau_{10}^*}\overline{q}(0)e^{-i\omega_{10}^*\tau_{10}^*\theta} + M_1 e^{2i\omega_{10}^*\tau_{10}^*\theta},$$
$$W_{11}(\theta) = -\frac{ig_{11}}{\omega_{10}^*\tau_{10}^*}q(0)e^{i\omega_{10}^*\tau_{10}^*\theta} + \frac{i\overline{g}_{11}}{\omega_{10}^*\tau_{10}^*}\overline{q}(0)e^{-i\omega_{10}^*\tau_{10}^*\theta} + M_2. \tag{B.8}$$

Here $M_1 = (M_1^1, M_1^2, M_1^3)^T \in R^3$ and $M_2 = (M_2^1, M_2^2, M_2^3)^T \in R^3$ are also constant vectors and can be determined by the following equations, respectively.

$$\begin{pmatrix} 2i\omega_{10}^* + \frac{\alpha x^*}{z^*}e^{-2i\omega_{10}^*\tau_{10}^*} & x^* & -\frac{\alpha x^{*2}}{z^{*2}}e^{-2i\omega_{10}^*\tau_{10}^*} \\ -\beta y^* & 2i\omega_{10}^* - \frac{\delta y^*}{(\sigma+y^*)^2} + \frac{y^*}{z^*}e^{-2i\omega_{10}^*\tau_2} & -\frac{y^{*2}}{z^{*2}}e^{-2i\omega_{10}^*\tau_2^*} \\ \varepsilon z^* & \mu z^* & 2i\omega_{10}^* \end{pmatrix} M_1 = 2\begin{pmatrix} Q_1 \\ Q_2 \\ Q_3 \end{pmatrix},$$

$$\begin{pmatrix} -\frac{\alpha x^*}{z^*} & -x^* & \frac{\alpha x^{*2}}{z^{*2}} \\ \beta y^* & \frac{\delta y^*}{(\sigma+y^*)^2} - \frac{y^*}{z^*} & \frac{y^{*2}}{z^{*2}} \\ -\varepsilon z^* & -\mu z^* & 0 \end{pmatrix} M_2 = -\begin{pmatrix} P_1 \\ P_2 \\ P_3 \end{pmatrix}, \tag{B.9}$$

with

$$\begin{aligned}
Q_1 =& h_4 q_3^2 e^{-2i\omega_{10}^*\tau_{10}^*} + h_3 q_3 e^{-i\omega_{10}^*\tau_{10}^*} + h_1 q_2, \\
Q_2 =& (k_4 q_2 q_3 + k_5 q_3^2)e^{-2i\omega_{10}^*\tau_2} + (k_3 q_2^2 + k_4 q_2 q_3)e^{-i\omega_{10}^*\tau_2} + k_2 q_2^2 + k_6 q_2^2 + k_1 q_2, \\
Q_3 =& l_1 q_2 q_3 + l_2 q_3, \\
P_1 =& 2h_4\overline{q_3}q_3 + (h_3\overline{q_3} + h_3 q_3)e^{-i\omega_{10}^*\tau_{10}^*} + 2\Re(h_1 q_2), \\
P_2 =& (k_4 q_3\overline{q_2} + k_4 q_2\overline{q_3} + 2k_5 q_3\overline{q_3} + k_3 q_2\overline{q_2}(e^{-i\omega_{10}^*\tau_2} + e^{i\omega_{10}^*\tau_2}) + k_4\overline{q_2}q_3 e^{-i\omega_{10}^*\tau_2} + k_4 q_2\overline{q_3}e^{i\omega_{10}^*\tau_2} \\
& + 2(k_2 + k_6)q_2\overline{q_2} + k_1\overline{q_2} + k_1 q_2), \\
P_3 =& l_1\overline{q_2}q_3 + l_1 q_2\overline{q_3} + l_2\overline{q_3}l_2 q_3.
\end{aligned}$$